Characterisation of Rotavirus strains responsible for breakthrough diarrhoeal disease among Zambian children using Whole Genome Sequencing

by
Innocent Mwape

Thesis presented in partial fulfilment of the requirements for the degree of
Master of Science (Medical Virology) in the Faculty of
Medicine and Health Sciences at
Stellenbosch University

Supervisor: Prof Corena de Beer
Co-supervisor: Dr Michelo Simuyandi

March 2024

Declaration

By submitting this thesis electronically, I declare that the entirety of the work contained therein is my own, original work, that I am the sole author thereof (save to the extent explicitly otherwise stated), that reproduction and publication thereof by Stellenbosch University will not infringe any third-party rights and that I have not previously in its entirety or in part submitted it for obtaining any qualification.

March 2024

Abstract - English (max. 500 words)

Background

Genetically altered viruses or variants have the potential to increase their virulence, pathogenicity, transmission, and ability to evade both natural and vaccine-induced immune responses leading to diarrhoeal disease in under five-year-old children who have received all recommended doses of Rotavirus (RV) vaccines, also known as breakthrough infections. Studies characterising RV strains responsible for breakthrough infections are rare in resource-limited countries like Zambia where RV-associated diarrhoeal disease is endemic. We aimed to characterise RV strains detected in fully vaccinated under five-year-old children residing in Zambia using next generation sequencing.

Methods

This was a case study nested under an open label randomised controlled RV vaccine clinical trial that evaluated safety and immune boosting effects of a third dose of Rotarix compared to a two-dose schedule. The Rotaclone kit was used to screen for RV in stool. We performed VP7 and VP4 genotyping on RV positive stool using Sanger sequencing. Whole genome sequencing was done on the Illumina Miseq platform. Genome assembly was done using Geneious software and multiple sequence alignment using Muscle in MEGA version 6.

Results

A total of 76 diarrhoeal stool specimens were collected and screened for RV of which 4/76 (5.2%) were positive. Genotypes of three of the four cases were identified as G1P[4], G12P[4] and G12P[8] using Sanger sequencing. Whole genome analysis revealed that the RVA/Human-wt/ZMB/CIDRZ-RV2088/2020/G1P[4]-I2-R2-C2-M2-A2-N2-T2-E2-H2 and RVA/Human-wt/ZMB/CIDRZ-RV2106/2020/G12P[4]-I1-R2-C2-M2-A2-N1-T2-E1-H2 strains were mostly DS-1-like with mono and multiple reassortant respectively, whilst the RVA/Human-wt/ZMB/CIDRZ-RV2150/2020/G12P[8]-I1-R1-C1-M1-A1-N1-T1-E1-H1 was a typical Wa-like strain. Comparison of VP7 antigenic epitope of strains causing breakthrough infections and Rotarix vaccine strains revealed several amino acid differences like G96P and M217E. Comparison of P[4] strains with VP4 of the Rotarix vaccine strain demonstrated two amino acids differences (P114Q and V115T) were P114Q is an immune escape mutation.

Discussion and Conclusion

Differences observed in amino acids in antigenic epitope suggested its role in the immune evasion of neutralising antibodies elicited by the vaccine. Findings from this study have potential to inform national RV vaccination strategies and the design of highly efficacious universal RV vaccines. Furthermore, there might be need to monitor strains that have escaped vaccine-induced immunity to prevent diarrheal diseases in children under five years of age.

Keywords: Rotavirus, Vaccine, breakthrough, Zambia, children, Reassortment

358 words

Opsomming - Afrikaans (max. 500 words)

Agtergrond

Geneties veranderde virusse of variante het die potensiaal om hul virulensie, patogenisiteit, oordrag en vermoë te verhoog om beide natuurlike infeksie en entstof-geïnduseerde immuunreaksies te ontduik wat lei tot diarree by kinders onder vyf jaar oud wat al die aanbevole dosisse Rotavirus (RV) entstowwe ontvang het, ook bekend as deurbraakinfeksies. Studies wat RV-stamme kenmerk wat vir deurbraakinfeksies verantwoordelik is, is skaars in hulpbronbeperkte lande soos Zambië waar RV-geassosieerde diarreesiekte endemies is. Ons het ten doel gehad om RV-stamme wat opgespoor is in volledig ingeënte kinders onder vyf jaar in Zambië woonagtig is, te karakteriseer met behulp van volgende generasie volgordebepaling.

Metodes

Hierdie studie is deel van 'n oop-etiket gerandomiseerde kliniese proef oor RV-entstof wat die veiligheid en immuunversterkende effekte van 'n derde dosis Rotarix in vergelyking met 'n twee-dosis skedule geëvalueer het. Die Rotaclon-stel is gebruik om stoelgang te sondersoek vir die teenwoordigheid van RV. Ons het VP7 en VP4 genotipering op RV positiewe stoelgang monsters uitgevoer deur gebruik te maak van Sanger volgordebepaling. Heelgenoomvolgordebepaling is op die Illumina Miseq-platform gedoen. Genoomsamestelling is gedoen met behulp van Geneious sagteware en meervoudige volgorde-belyning met behulp van Muscle in MEGA weergawe 6.

Resultate

'n Totaal van 76 diarree-stoelgangmonsters is versamel en getoets vir RV waarvan 4/76 (5.2%) positief was. Genotipes van drie van die vier gevalle is geïdentifiseer as G1P[4], G12P[4] en G12P[8] deur gebruik te maak van Sanger-volgordebepaling. Heelgenoomanalise het aan die lig gebring dat die RVA/Human-wt/ZMB/CIDRZ-RV2088/2020/G1P[4]-I2-R2-C2-M2-A2-N2-T2-E2-H2 en RVA/Human-wt/ZMB/CIDRZ-RV2106/2020/G12P[4]-I1-R2-C2-M2-A2-N1-T2-E1-H2 meestal DS-1-agtige stamme was met onderskeidelik mono- en veelvuldige reassortante, terwyl die RVA/Human-wt/ZMB/CIDRZ-RV2150/2020/G12P[8]-I1-R1-C1-M1-A1-N1-T1-E1-H1 'n tipiese Wa-agtige stam was. Vergelyking van VP7-antigeniese epitoop van stamme wat deurbraakinfeksies veroorsaak, en Rotarix-entstofstamme het verskeie aminosuurverskille soos G96P en M217E aan die lig gebring. Vergelyking van P[4]-stamme met VP4 van die Rotarix-entstofstam het twee aminosureverskille (P114Q en V115T) gedemonstreer, waar P114Q 'n immuunontsnappingsmutasie is.

Bespreking en Slot

Verskille waargeneem in aminosure in antigeniese epitoop het die rol daarvan voorgestel in die immuunontduiking van neutraliserende teenliggaampies wat deur die entstof ontlok word. Bevindinge van hierdie studie het potensiaal om nasionale RV-inentingstrategieë en die ontwerp van hoogs doeltreffende universele RV-entstowwe in te lig. Verder kan dit nodig wees om stamme te monitor wat entstofgeïnduseerde immuniteit vrygespring het om diarreesiektes by kinders jonger as vyf jaar te voorkom.

370 woorde

Acknowledgements

- Jehovah God for granting me the strength, opening the opportunity to learn and completion of the master's degree work;
- David Ojok, the Laboratory Director has been instrumental in helping to get the reagents and permitting to carry out this work in his Laboratory;
- Prof. Corena De Beer, thank you for taking your precious time to mentor and review this work;
- Michelo Simuyandi and Natasha Makabilo Laban grateful for the permission to work on the ROVAS 2 clinical trial specimen;
- Grateful to the Children and guardians/parents for participating in the study.

Table of Contents

List of Figures:

List of Tables

List of Abbreviations

BIC	Bayesian Information Criterion
BLAST	Basic Local Alignment Search Tool
BLT	Bead-linked Transposomes
BV-BRC	Bacterial Viral Bioinformatic Resource Centre
cDNA	Complementary Deoxyribonucleic Acid
CIDRZ	Centre of Infectious Diseases Research in Zambia
DLP	Double Layered Particle
DNA	Deoxyribonucleic Acid
ds	double-stranded
HBGA	HistoBlood Group Antigens
Ig	Immunoglobulin
IL	Interleukin
IPB	Illumina Purification Beads
LMIC	Low Middle Income Countries
MDA	Melanoma Differentiation-Associated genes
NaOH	Sodium Hydroxide
NCBI	National Centre for Biotechnology Information
NSP	Non-Structural Proteins
ORF	Open Reading Frame
PBS	Phosphate Buffered Saline
PCR	Polymerase Chain Reaction
PRR	Pattern Recognition Receptor
RCWG	Rotavirus Classification Working Group
RdRNA	RNA dependent RNA Polymerase
RIG	Retinoic Acid-Inducible Genes

RNA	Ribonucleic Acid
RT-PCR	Reverse Transcription Polymerase Chain Reaction
RV	Rotavirus
RVA	Rotavirus Group A
RV-AGE	Rotavirus acute gastroenteritis
sIg	Secretory Immunoglobulin
SSA	Sub Saharan Africa
ss	single-stranded
TLR	Toll-like Receptor
U5	Under five-year-old
UNZABREC	University of Zambia Biological Research Ethics Committee
UTR	Untranslated Region
USA	United States of America
VP	Viral Proteins
WGS	Whole Genome Sequencing
WHO	World Health Organisation

Research Dissemination

- Accepted to MDPI Vaccines Journal
- Abstract accepted as e-poster presentation at African Rotavirus Symposium to be held in Lagos, Nigeria November 2023

Other Research work participated during the course work

- Laban NM, Bosomprah S, Simuyandi M, Chibuye M, **Mwape I,** Chauwa A, Chirwa-Chobe M, et al. Evaluation of ROTARIX® Booster Dose Vaccination at 9 Months for Safety and Enhanced Anti-Rotavirus Immunity in Zambian Children: A Randomised Controlled Trial. Vaccines (Basel). 2023 Feb 3;11(2):346.
- Adriace Chauwa, Natasha Makabilo Laban, Samuel Bosomprah, Bernard Phiri, Mwelwa Chibuye, Obvious Nchimunya Chilyabanyama, Sody Munsaka, Michelo Simuyandi, **Innocent Mwape,** Cynthia Mubanga, Masuzyo Chirwa, Caroline Chisenga, Roma Chilengi. Maternal and infant histo-blood group antigens (HBGA) profiles and its influence on oral rotavirus vaccine (ROTARIX®) immunogenicity among infants in Zambia. Vaccines (Basel). Received: 24 May 2023

CHAPTER ONE: INTRODUCTION

1.1 Background

Group A rotaviruses (RVA) are responsible for 1.76 million hospitalisations among under five-year-old (U5) children worldwide, with a quarter of these cases occurring in Sub-Saharan Africa (1). In Zambia, 15 000 rotavirus (RV)-related deaths occur among children U5 annually making RV the third most common cause of death among children (2).

RV is transmitted mainly via a faecal-oral route with an infectivity dose as low as 10 viral particles, making RV highly contagious (3). In an infected host, RV has an incubation period of between two to four days, followed by manifestation of disease, including fever, vomiting and subsequent watery stool. Prolonged vomiting and watery stool are common symptoms, particularly in children, and causes severe dehydration which may be fatal (4) .

The RV genome consists of 11 segments encoding six non-structural proteins (NSP1, NSP2, NSP3, NSP4, NSP5/NSP6) and six structural viral proteins (VP), namely VP1, VP2, VP3, VP4, VP6 and VP7 (5,6). The evolution of RV has been associated partly by error-prone ribonucleic acid (RNA) dependent RNA (RdRNA) Polymerase during replication as well as segmented nature of the 11 genes of the RV genome, which result in reassortment of genes from different genogroups (7). The conventional RV classification has been based on two surface proteins, the VP7 (a glycosylated outer capsid protein representing G genotype) and VP4 (a protease sensitive protein for P genotype) (8). VP7 and VP4 induce neutralising antibodies important for the immune protection and used for the viral serotyping (9). Based on the binary classification the following have been reported as the most prevalent genotypes globally, G1P[8], G2P[4], G3P[8], G4P[8] and G9P[12], accounting for about 90% of RV genotypes (10).

The RV Classification Working Group (RCWG) recommended the classification of RVs based on the whole genome constellation of all 11 segments RV as follows: Gx-P[x]-Ix-Rx-Cx-Mx-Ax-Nx-Tx-Ex-Hx, where x represented the genotype number and the letter denoted the functional name of the gene (11). Based on full genome studies, it has been possible to elucidate the reassortment events between different genogroups, interspecies transmission of the genome segment as well as critical in understanding genetic relationship and pattern of RV evolution and also monitoring the vaccine effectiveness (11,12).

The deployment of RV vaccines in the immunisation programmes of several countries globally has resulted in a substantial decline in the burden of RV-related severe acute gastroenteritis (RV-AGE) among children U5 (13). Currently, four RV vaccines, Rotarix (GlaxoSmithKline, UK), Rotateq (Merck, USA), Rotavac (Bharat Biotech, India) and Rotasiil (Serum Institute of India), received approval from the World Health Organisation (WHO). Rotarix is an oral, monovalent, live attenuated human RV G1P[8] strain administered to children as two doses (14). Rotateq is an oral, pentavalent vaccine consisting of live, attenuated human and bovine reassortant RV strains (G1, G2, G3, G4 and P[8]) and administered to children as three doses (15). Rotavac is an oral liquid frozen monovalent vaccine composed of human RV strain 116E G9P[11] which was isolated from a neonate in India in 1986 (16). Rotasiil is an oral heat-stable pentavalent vaccine composed of five live attenuated reassortant RVs of human and bovine strains (G1, G2, G3, G4 and G9) administered as a three-dose regimen (17).

Despite the reduction in the RV gastroenteritis due to the introduction of the oral RV vaccines in several countries, breakthrough strains continue to pose a threat to the reduction of the RV-AGE among children U5. Furthermore, a study in Japan conducted to understand the cause of diarrhoea among vaccinated children detected vaccine-derived strains although other enteropathogens were also found (18). On the other hand, the study in Belgium reported breakthrough RV strains as the causative agent of diarrhoea in 54% of infants with diarrhoea detected with vaccine reassortants as responsible for the breakthrough diarrhoeal disease (19). The study conducted by Ogden and colleagues in the United States of America (USA) found that the mismatch in the antigenic epitopes between the vaccine VP7 and VP4 as well as the predominance of genotype not included in the vaccine as the main drivers of RV strains responsible of causing diarrhoea among the vaccinated infants (20). Therefore, a small percentage of children who have received all recommended doses (fully vaccinated) of RVA vaccines can sometimes be reinfected with vaccine and non-vaccine RVA strains. We defined all RVA infections occurring in children after full vaccination as breakthrough infections.

Breakthrough infections are mainly caused by genetic difference in strains (21). Genetically altered strains might demonstrate enhanced capabilities such as transmission, increased virulence and/or pathogenicity leading to higher rates of hospitalisation, morbidity, and mortality; and might acquire the ability to escape both natural and vaccine-induced immunity (21). The threat of RVA breakthrough to public health and the economy especially in endemic regions cannot be emphasised enough. Characterising RVA strains causing breakthrough infections using whole

genome sequencing (WGS) has significant implications for vaccination strategies and the design of highly effective next-generation RVA universal vaccines. Additionally, studies addressing RVA breakthrough infections in developing countries are extremely rare justifying the need to conduct this study.

1.2 Statement of the problem

The RV strains responsible for causing breakthrough infections pose a threat to further reduction of RV-AGE among children U5 in low middle income countries (LMIC), including Zambia. Furthermore, studies on breakthrough infections are rare in most developing countries where the burden of RV is high. Several RV genotype surveillance studies conducted in sub-Saharan African (SSA) countries have been performed with the conventional genotyping of VP7 and VP4, with genotype distribution ranging from the mixed genotypes to untypable strains (22). The limited information generated from use of VP4 and VP7 on the genetic diversity of RVs in SSA has provided an information gap on the whole genome constellation of the circulating RVs.

1.3 Significance of the study

Characterising RVA variants causing breakthrough infections using WGS has significant implications for improvement of vaccination strategies and the design of highly effective next-generation RVA vaccines. Furthermore, few studies are addressing RVA breakthrough infections in LMIC, justifying the need to conduct this study.

1.4 Research question

What is the genetic distinct feature of RV strains responsible for breakthrough diarrhoeal diseases among vaccinated children in Zambia?

1.5 Study aim

The aim of this study was to comprehend the genetic distinct features of each of the 11 genes of RV strains causing the breakthrough infections among vaccinated infants.

1.6 Specific objectives

The aim of the study was attained through the following specific objectives:

i. Detection of RV in fully vaccinated children who presented with diarrhoea with subsequent determination of the VP7 and VP4 genotype;

ii. WGS of the RV using Illumina Miseq;

iii. Identification of genetic distinct features of RV strains infecting fully vaccinated children by using phylogenetic analysis; and

iv. Comparison of antigenic epitope of VP7 and VP4 of RV strains responsible of breakthrough diarrhoea among vaccinated children.

CHAPTER TWO: LITERATURE REVIEW

2.1 Epidemiology and classification of rotaviruses

Globally, more than 128 000 children U5 died of RV diarrhoea and 66.3% of these deaths occurred in SSA in 2016 (23).

RV belongs to the family of reoviridae, genus *rotavirus* (5). RVs consist of three concentric layers with the inner layer housing the 11 segments of the double-stranded (ds) RNA of the genome. The VP6 protein forms the intermediate capsid of the virus. Historically, serological techniques have been used in the classification of RVs. The VP6 is highly immunogenic, thereby inducing antibodies which appears first after infection (24). Based on the antigenic epitopes of the VP6, RV has been classified in to nine serogroups, A to I (25). The genetic reassortment has been shown not to occur between the different RV serogroups (26). Groups A, B and C have been associated with infection in humans (26). Group A remains the major cause of diarrhoea among children U5 globally, whereas group B has been associated with infection in all age groups (27).

The distinct antigenic epitope in VP6 within serogroup A has led to subdivision into the subserogroups, such as subgroup I, subgroup II, subgroup I+II and non-I, non-II (28). The outer surface viral proteins the (VP7 and VP4) induce the neutralising antibodies used for RV serotyping. The antigenic epitope of VP7 defined the G types, whereas the VP4 protease sensitive defined the P serotypes (29). There exists high correlation between the G serotype and G genotype. However, the P serotype and P genotype have shown poor correlation; this has been attributed to cross-reactivity within the P serotypes making P serotyping complex (30). The complication with P serotyping has resulted in double classification for P, with a number which has no square bracket indicating serotype, whereas P with a number in square bracket denoted genotype (31).

The binary classification of RV based on G/P genotyping has been limited as it left out the information on the nine segments of the RV genome. To bridge this gap, the RCWG recommended RV classification based on the nucleotide percentage cut-off value to assign genotype to each of the 11 segments of the RV genome. The complete genetic genotype of RV based on the whole genome is represented by Gx-P[x]-Ix-Rx-Cx-Mx-Ax-Nx-Tx-Ex-Hx, where X denoted the number of the genotype, whereas the letter indicated the gene encoding segments G(VP7)-P(VP4)[x]-I(VP6)x-R(VP1)x-C(VP2)x-M(VP3)x-A(NSP1)x-N(NSP2)x-T(NSP3)x-E(NSP4)x-H(NSP5/6)x (11).

Three major human RV strains have been found to have common origin with animal RVs. For example, the human Wa-like genogroup has common origin with the porcine RVs, the human DS-1-like genogroup has common origin with the bovine RVs and the AU-1-like human genogroup has the common origin with the canine and feline RVs (32).

2.2 Structure of rotavirus

Due to burden of acute gastroenteritis among children U5 in Australia in 1973, Ruth Bishop and co-workers (33) obtained ultrathin sections of the duodenal mucosa from children with acute gastroenteritis. When examined under the negative stain electron microscope, these sections revealed abundant wheel-like particles in the enterocytes lining the upper villi surface as shown in Figure 1a.

The name RV was derived from the Latin word Rota meaning wheel (33). The mature infectious virus consists of three recognised protein layers. See Figure 1b. The first single layered particle comprises of 120 molecules of VP2 forming the core capsid. The core capsid encloses replication enzyme, the RNAdRNA (VP1), methyl transferase (VP3) a capping enzyme and the 11 segments of the genome of the dsRNA (34). The double layered particle encases the core capsid with intermediate capsid consisting of 780 molecules of VP6, which make contact with the VP2, VP7 and VP4 (34,35). The mature virus consists of the VP7 and VP4 which enclose the double layered particle (36). Due to the presence of trypsin in the small intestine VP4 is cleaved into two subunits, the VP8 and VP5. The VP5 forms the stalk of the spike protein which is partly embedded in the VP7 and makes contact with VP6, whereas the VP8 corresponds to the distal head of the VP4 (37,38), as shown in Figure 2.

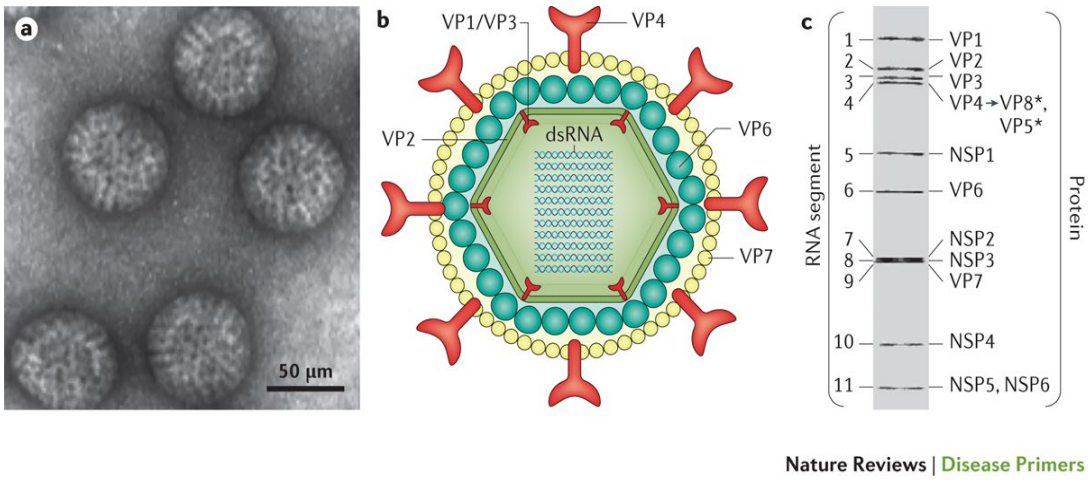

Figure 1: Structure of Rotavirus. Adapted from Crawford, S. et al., (2017). Rotavirus infection. Nat Rev Dis Primers 3, 17083 (2017)

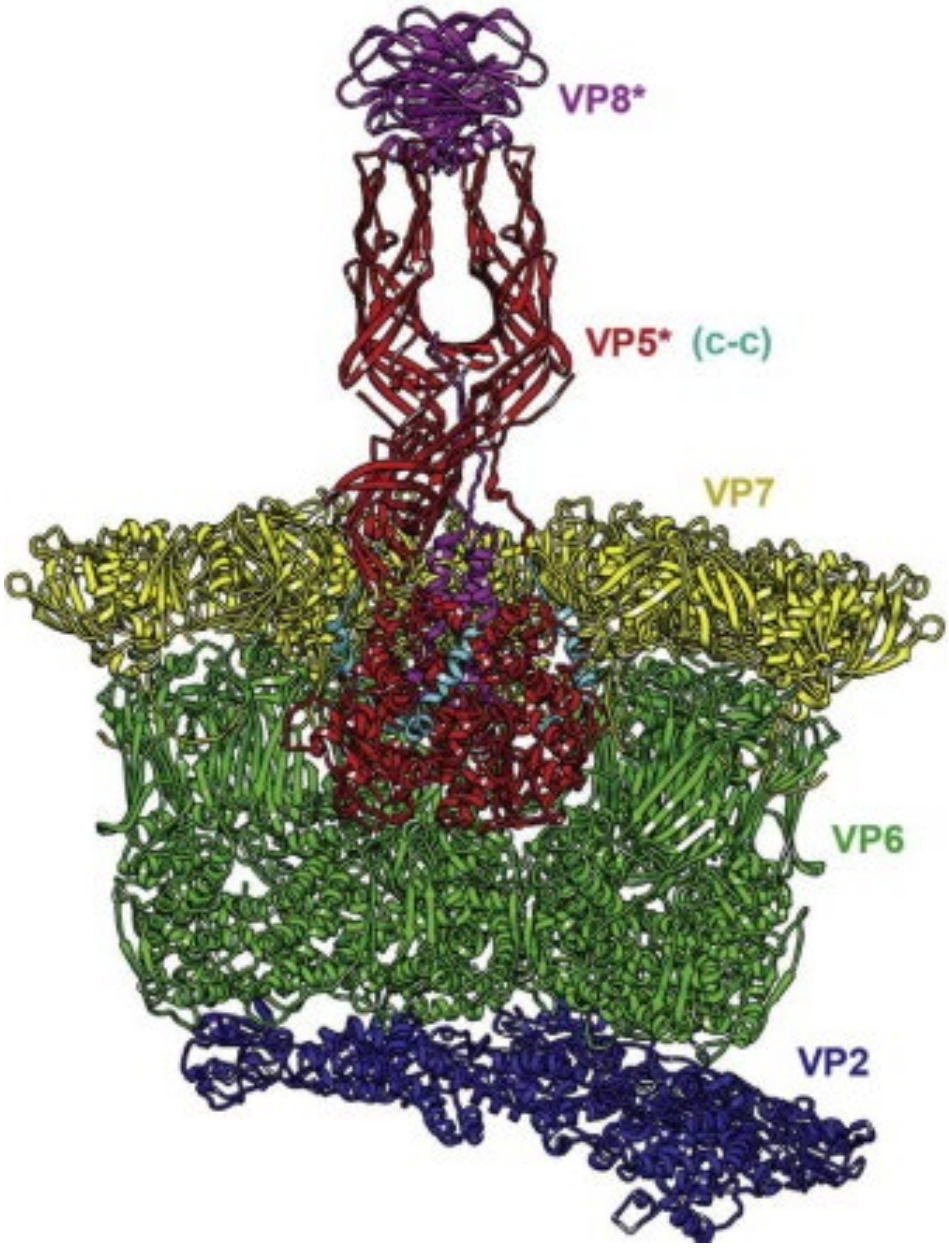

Figure 2: Structure of RV capsid proteins. Adapted from Settembre et al., (2011).

2.3 Genomic structure

The RV genome consists of 11 segments of dsRNA. The size of each segment range from 667 to 3 302 base pairs (5). Each of the 11 segments have a conserved sequence at the 5'-terminal consisting of Guanidine followed by the Untranslated Region (UTR), then Open reading frame (ORF) and finally the 3'-terminal with conserved sequence of cytidine (40). The conserved 3'-end sequence acts as transcriptional initiation signal (40). Each of the 11 segments has a single ORF with the exception of the segment 11, which has a bicistronic encoding the NSP5 and NSP6 (41). Table 1 below described the gene name and protein encoded.

Table 1: Rotavirus genomic segments

Genome Segment	Size (bp)	Encoded Protein	Protein Size (kDa)	Name of Protein	Number of Molecules per Virion
1	3302	VP1	125	RdRNA polymerase	12
2	2687	VP2	94	Core Capsid	120
3	2592	VP3	88	Methyltransferase	12
4	2362	VP4	86	Spike protein	180
5	1581	NSP1	58	Non-structural Protein	
6	1356	VP6	44	Intermediate Capsid	780
7	1062	VP7	37	Outer Capsid	780
8	1059	NSP2	36	Non-structural protein	
9	1074	NSP3	34	Non-structural protein	
10	751	NSP4	20	Non-structural protein	
11	666	NSP5	21	Non-structural protein	
		NSP6	12	Non-structural protein	

2.4 Rotavirus replication cycle

RV infects and replicates in the mature enterocytes in the upper portion of the villi depending on the cell receptors (41). The presence of trypsin in the small intestine lead to proteolytic cleavage of the VP4 into VP5 and VP8. The VP8 has the initial interaction with cellular receptors (42). The animal RV strains usually bind to the sialoglycans such as gangliosides GM1 and GD11 as receptors (43). The viral strains infecting humans deploy several host receptors such as the HistoBlood Group Antigens (HBGA) to which some humans have been shown to be susceptible or resistant depending on the virus P genotype and host genetic composition (43). Viral internalisation into the mature enterocytes occur via the endocytic pathway or direct penetration, as shown Figure 3C. The endocytic pathways internalise the virus via clathrin dependent or -independent depending on the virus strain (44). The Wa-like and DS-1 strains have been shown to use the clathrin-dependent

pathways (44). The engulfed virus in the endosome lose the viral surface proteins VP7 and VP4 due to the low pH and calcium in the endosome, which lead to the release of the transcriptionally active Double Layered particles (DLP) in the cytoplasm (45,46). The presence of DLP in the cytosol activates the transcription complex of RdRNA polymerase (VP1) as well as capping enzyme (VP3) which results in synthesis of single-stranded (ss) RNA required for the synthesis of VPs and template for genome replication Figure 3B.

Viroplasms formed in the cytoplasm, house the synthesis of VPs and assembly (45). They consist of viral RNA, viral and cellular proteins, surrounded by the lipid droplet. The packaging of viral RNA and proteins occur in the viroplasm with the budding of DLP with NSP4 playing a role as intracellular receptor for DLP budding into the endoplasmic reticulum where final maturation occurs by loss of lipid and encasing the virus with VP4 and VP7 (47).

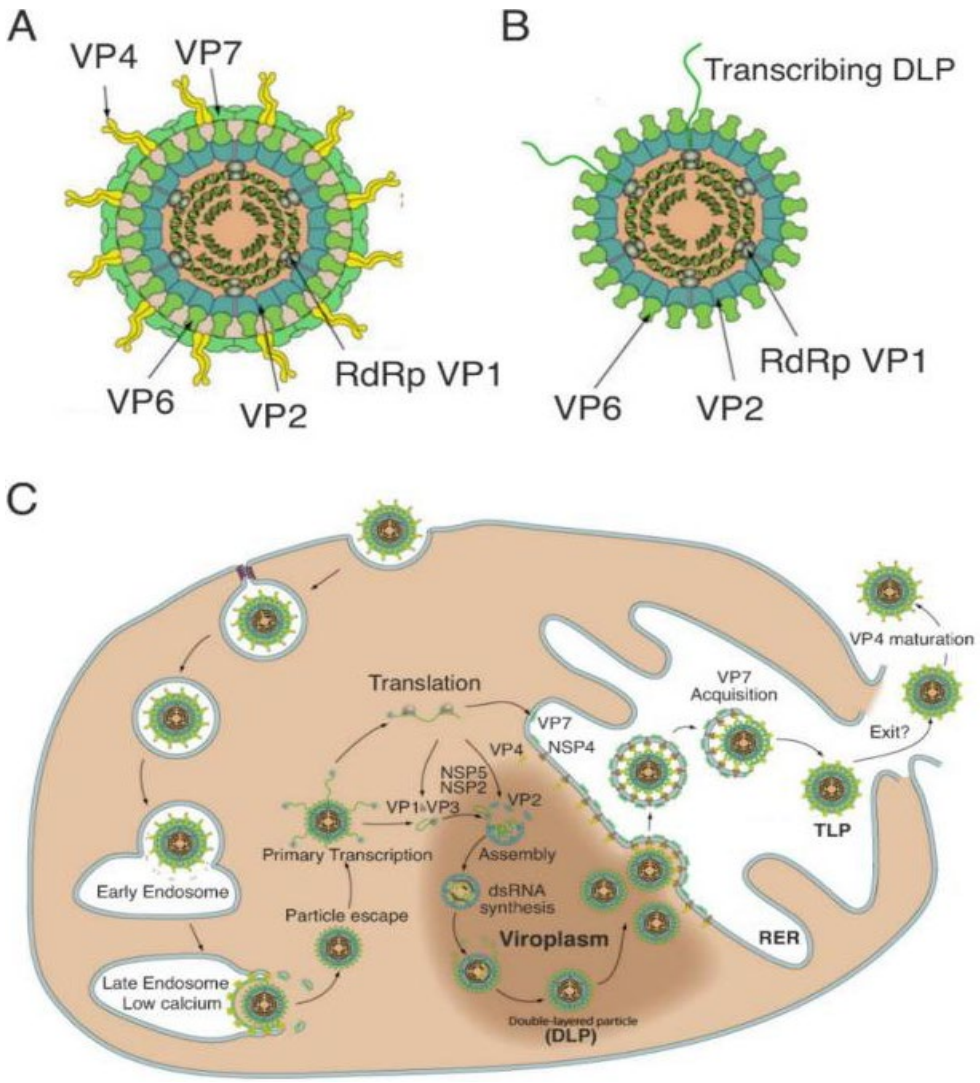

Figure 3: Rotavirus Replication cycle. Adapted from Papa, G. et al., (2021). Assembly and Functions of rotavirus Replication Factories.

2.5 Transmission of rotavirus and pathophysiology

Infectious RV has a stable triple layered structure enabling survival in the environment for several weeks and for about four hours on human hands (48) [73]. The reported RV infectivity dose ranged from 10-1 000 particles with high shedding of the virus of 10^{11} particles per gram of stool before the onset of symptoms and for weeks afterward, making RV highly contagious (3). The virus mainly transmits via the faecal-oral route by contact with contaminated surfaces and infected individuals shedding the virus (3). It has an incubation period of about 1-4 days before onset of symptoms. Children infected with RV often manifest with high fever (49), which is indicative of an initial response of the immune system which is regulated by the hypothalamus. The cytokines observed in high levels in children infected with RV and suggested to trigger stimulation of the hypothalamus and afferent sensory nerves include interleukin (IL)-6, IL-1beta as well as Tumour necrosis factor (50). Children with RV infection manifest with non-bloody diarrhoea.

There are two suggested mechanisms by which RV infection can cause diarrhoea (51); firstly, by disruption of enterocytes lining the surface of the upper villi which resulted in malabsorption and osmotic diarrhoea, and secondly, by triggering the enterotoxin NSP4 which activates the phospholipase C, leading to increased intracellular calcium. This results in activation of calcium dependent chloride channels, with subsequent increase of electrolytes in the lumen (52). RV infection in children U5 has been associated with vomiting , suggesting that RV also infects the small intestinal enteroendocrine cells, such as the enterochromaffin cells, which further secrete serotonin and activate the enteric nervous system and extrinsic vagal afferent neurons with subsequent stimulation of the Nucleus tractus solitarious and postrema area of the brain leading to vomiting in children (53).

2.6 Immunity

The immune response against RV involves both the innate and adaptive immunity (54). The innate immunity components that provide defence against RV infection include expression of receptors such as HBGA, as well as reduced viral infectivity when the VP4 is cleaved by trypsin (54). Furthermore, the enterocytes lining the surface of the villi contain the Pattern Recognition Receptors (PRR), such as Toll-like receptor (TLR) 3, retinoic acid-inducible gene (RIG)-I and melanoma differentiation-associated protein (MDA) 5 which initially recognises the RV dsRNA and trigger the secretion of type 1 and 3 interferons which aid in viral clearance (54). The RV infection engulfed by M cells, present the antigen to dendritic cells which process the RV antigen and present

to the T helper 2 cells in the Peyer patches in the presence of transforming growth factor beta 1. IL-4 leads to class switching deoxyribonucleic acid (DNA) recombination and activation of the antigen immunoglobulin (Ig) A-specific B cells which then migrate to the lamina propria and differentiate into specialised plasma B cells which secrete antigen-specific Ig G and IgA. The Ig polymeric receptor at the basal intestinal epithelial layer facilitates the translocation of IgA into the lumen as secretory Ig (sIg) A (55). The serum IgA levels have been shown to correlate with protection against RV infection (56)[87]. VP4 and VP7 induce neutralising antibodies which mediate both heterotypic and homotypic protection (57). The induced RV-specific T cells have been shown to play a critical role in RV clearance (58).

2.7 Rotavirus vaccines

Globally, deployment of RV vaccines has led to the decline of RV mortality among children U5 (13). More than 100 countries have already incorporated the RV vaccination in their national immunisation programmes (13).

Currently, four oral RV vaccines have received WHO prequalification licensure. Firstly, RotaTeq (Merck & Co., Inc., Kenilworth, NJ) received WHO prequalification in 2008. It is an oral live attenuated pentavalent vaccine which composed of five reassortant viruses of human and bovine origin (59). The first four reassortant viruses of the vaccine contained the surface protein combinations of VP7 outer capsid protein of four human serotypes (G1, G2, G3 and G4) and the VP4 spike protein from bovine strain P[5]. The fifth reassortant virus consists of the VP7 from G6 serotype of bovine origin and VP4 spike protein from strain P1A [8] of human origin (60). The reported efficacy of Rotateq in developed countries was higher than 95% whereas in LMIC the efficacy was less than 60%. Furthermore, the vaccine provides both heterotypic and serotype-specific protection among children U5 (61). Rotarix vaccine is a monovalent G1P8 of human strain manufactured by GlaxoSmithKline Biologicals, Rixensart, Belgium. It is a two-dose oral vaccine administered to infants between 6 and 12 weeks of age.

In 2018 two other oral RV vaccines manufactured in India received WHO prequalification and subsequent recommendation for incorporation in the national immunisation programmes. Rotavac (Bharat Biotech International Ltd., Hyderabad, India) is a monovalent vaccine of human strain G9P[11] with reported efficacy of 56% in both India and Zambia among children with severe gastroenteritis (62). Rotasiil (Serum Institute of India Pvt. Ltd., Pune, India) is a lyophilised heat-stable live attenuated pentavalent vaccine with reassortant human and bovine strains (G1, G2, G3,

G4 and G9). Evidence from clinical trials conducted in India and Niger has shown efficacy of 39-55% among children with severe gastroenteritis (63).

2.8 Rotavirus genetic diversity

Globally, there is rich RV genetic diversity of strains causing severe diarrhoea among children U5. It has been observed that developed countries have less RV genetic diversity, usually limited to four predominant strains of the G-P genotypes as G1P [8], G2P [4], G3P [8] and G4P[8], whereas developing countries have greater extensive genetic RV diversity, which include but is not limited to G1P [8], G2P [4], G3P [8], G4P [8], G1P [6], G2P [6], G3P [6], G8P [6], G9P[8] and G12P[8], as well as the mixed and untypable genotypes (64,65). The six years surveillance under the auspice of the Africa Rotavirus Network revealed the following genotypes has the most predominate strains before and after rotavirus vaccine introduction G1P[8] , G2P[4], G9P[8], G12P[8], G2P[6] and G3P[6] (64).Furthermore, this surveillance demonstrated atypical genotypes such as G1P[4], G2P[8],G9P[4] and G12P[4] attributed to reassortment (64).The high genetic diversity in SSA has been attributed to increased frequency of detection of mixed genotype co-infection (11-15%) of distinct genotypes of G-P (66). The G/P genotype classification has provided limited information on the genetic relationships and evolution dynamics of circulating RV as the genetic make-up in the other nine segments remains limited. To overcome this barrier the advancement in sequencing technology by use of next generation sequencing has enabled whole genome sequencing, as well as the recent whole genome classification by the RCWG that assigned genotypes to each of the 11 segments of the genome(11). The recent WGs studies conducted in SSA have revealed intergenogroup and interspecies reassortments among children with severe RV-AGE (66).

2.9 Breakthrough strains and vaccination

The primary natural RV infection in children U5 elicits neutralising antibodies, which provide protection against development of severe gastroenteritis in children during subsequent RV infection (67). The first RV infection induces predominantly serotype-specific neutralising antibodies, whereas subsequent infections trigger a heterotypic response (68). The secreted intestinal and serum neutralising antibodies have been shown to provide protection after natural infection in adult challenges (69). The four RV vaccines that are currently available are all live attenuated vaccines which mimic the natural infection in the protection against gastroenteritis. These vaccines have significantly contributed to the global decline in RV gastroenteritis hospitalisation among children U5, however, the strides made by the vaccine are being threatened by emergence of breakthrough

strains associated with severe RV-AGE in vaccinated children. A study by Simsek and colleagues (19) used WGS to demonstrate that breakthrough strains were causing severe gastroenteritis in vaccinated children, as well as some vaccine-reassortment. Another study conducted in Zambia by Simwaka and co-workers (2) have reported that both homotypic and heterotypic breakthrough strains were associated with severe diarrhoea in vaccinated children. Breakthrough infections are mainly caused by genetically altered (variant) strains (21). Variant strains may exhibit increased transmission capabilities; increased virulence and/or pathogenicity leading to higher rates of hospitalisation, morbidity, and mortality; and may acquire the ability to escape both natural and vaccine-induced immunity (21).

This study therefore aimed to characterise the RV strains responsible for breakthrough diarrhoea among fully vaccinated children in Zambia.

CHAPTER THREE: MATERIALS AND METHODS

3.1 Study design

This was a case study characterising the RV strains responsible of breakthrough infections among fully vaccinated children in Zambia.

3.2 Study participants

We used stool samples collected and tested for RV as part of a RV vaccine clinical trial conducted in Lusaka, Zambia. This trial evaluated the safety and immunogenicity benefits of an additional third dose of Rotarix vaccine administered at 9 months of age (70). Briefly, 214 infants aged 6 to 12 weeks were enrolled and followed up until 3 years of age. All infants received the routine two doses of Rotarix vaccine and at 9 months old, were randomised to receive a third dose of Rotarix measles/rubella concomitantly with measles/rubella vaccination (intervention arm) or receive only measles/rubella vaccine (control arm). In the first year of follow-up, 76 infants presented to the study clinic with acute diarrhoea and had a stool sample collected and stored at -20°C prior to testing. A total of 4 out of 76 (5.2%) stool specimens were RV positive by an enzyme immunoassay (Premier Rotaclone). Of these, three had sufficient stool specimen available for molecular analysis and were identified as G genotypes using VP7 based PCR assay on 1% agarose gel visualisation stained with gel red as 2 (two) G3 and 1 (one) G4 genotypes [70]. We then performed Sanger Sequencing on these 3 specimens for the VP7 and VP4 for the G and P genotypes, followed by WGS using Illumina Miseq platform. The study overview and flow chart are presented in Figure 4.

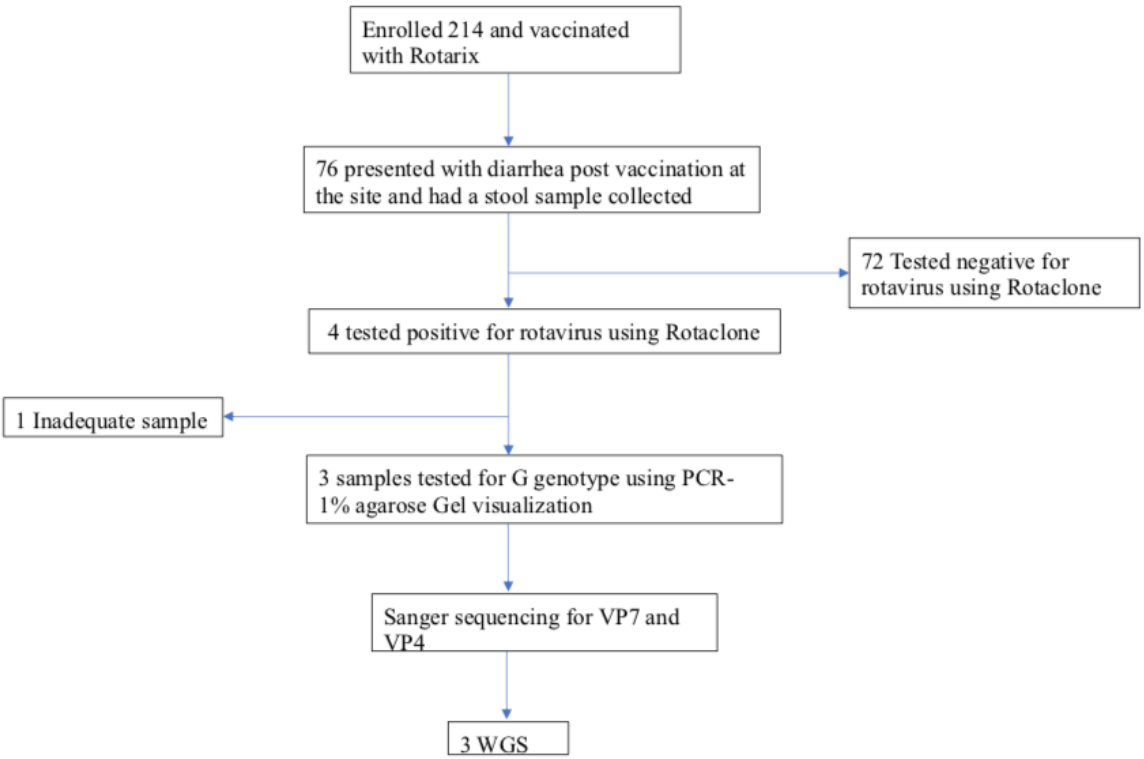

Figure 4: Study Flow Chart for the RV vaccine clinical trial conducted in Lusaka, Zambia.

3.3 Study site

The research project was conducted at the Centre of Infectious Disease Research in Zambia (CIDRZ) Laboratory in Lusaka, Zambia.

3.4 Sampling frame and sample size

This was a case study nested under open label randomised controlled trial evaluating safety and immunogenicity of ROTARIX® vaccine at 9-month infant age. In which we anticipated a 15% or greater increase in log10 RV-IgA response after third dose. Using a two-sample t-test, and assuming equal SD at 5% level of significance, we therefore required a total of 196 infants (98 per arm) to detect an increase to 3.13 log10 RV-IgA due to the booster dose of ROTARIX® at an 80% power. We made an upward sample size adjustment of 9% to account for potential loss to follow up to reach the total of 214 infants to be recruited in the study. The estimation was performed using Stata 14 MP “power" command (StataCorp™, College Station, Texas, USA). This study utilised clinical data and raw stool samples from children enrolled in a randomised controlled RV vaccine clinical trial and received two or three dose Rotarix vaccination at nine months of age. All the samples tested positive for the Rotavirus using the Premier Rotaclone kit were included in the study.

3.4.1 Inclusion criteria

- Children aged 6-12 weeks.
- Positive for RV and received vaccination.
- Adequate sample volume.
- Sample collected at least 15 days after second or third dose and episode of gastroenteritis;
- Presence of a complete written consent form from the parent/s.
- Matching clinical information.

3.4.2 Exclusion criteria

- Inadequate sample volume.
- Stool negative for RV.
- Incomplete or lack of consent from the parent/s.

3.5 Study laboratory procedures

3.5.1 Viral RNA extraction

Stool samples stored at -80°C were subjected to RNA extraction. The commercial Qiagen Viral RNA kit (Qiagen, GmbH, Hilden, Germany) was used for the extraction with minor modification in the pre-extraction stage as previous described (71). Briefly, 10% faecal suspension was prepared by adding a loopful or 100 µL of stool to 1 mL phosphate buffered saline (PBS), then mixed by vortexing for 5-10 minutes. This was followed by centrifugation at 4 000 rpm for 20 minutes, and subsequently using 140 µL of the supernatant for extraction. The procedure is summarised below.

Labelled the 1.5 mL tubes with Patient ID numbers inside a biological safety cabinet.

i. Pipet 560 µL of A Viral Lysis buffer (AVL) buffer containing the carrier RNA into a 1.5 mL tube.

ii. Add 140 µL of the 10% stool suspension. Mix by pulse-vortexing for 15 seconds.

iii. Incubate at room temperature for 10 minutes.

iv. Add 560 µL of ethanol (96-100%) to the sample, mix by pulse-vortexing for 15 seconds, then centrifuge briefly.

v. Transfer 700 µL of the solution to a spin column placed in a 2 mL collection tube. Centrifuge for 1 minute at (6 000 g or 8 000 rpm); then place the spin column into a clean 2 mL tube.

vi. Wash the column containing bound RNA with 550 µL of A Wash 1 buffer (AW1) buffer and centrifuge (at 6 000 g or 8 000 rpm) for 1 minute. Place column in a clean 2 mL collection tube.

vii. Wash the column with 550 µL of A Wash 2 buffer (AW2) buffer and centrifuge at full speed (20 000 g or 14 000 rpm) for 3 minutes.

viii. Dry spin for 1 minute at 20 000 g or 14 000 rpm.

ix. Place the spin column in a labelled 1.5 mL micro-centrifuge tube, add 50 µL A Viral Elution (AVE) buffer and elute the RNA at full speed.

3.5.2 Sanger sequencing of the VP7 and VP4

The primers used in reverse transcription (RT)-PCR was adapted from the previous published protocol (72), and modified by the use of different enzymes.

The procedure is summarised as follows:

i. Use 5 µL of extracted RNA and denature at 95^{o}C for 5 minutes.

ii. Perform the RT-PCR using One step SuperScript III with Platinum *Taq* High fidelity DNA polymerase kit (Invitrogen).

iii. The reaction contains 5 µL denatured RNA, 1 µL reverse primer(10µM), 1 µL forward primer (10µM), 25 µl 2X reaction mix, 1 µL enzyme mix and 17 µL of water.

iv. The reverse transcription reaction is then carried out at 50°C for 30 minutes.

v. The denaturation of reverse transcriptase and activation of the platinum *Taq* occur at 94°C for 2 minutes, followed by 40 cycles amplification according to the following thermocycling conditions:

- 15 seconds at 94°C.
- 30 seconds at 45°C.
- 3.5 minutes at 68°C for VP4 and 1.5 minutes at 68°C for VP7.

The PCR products were visualised on a 1% agarose gel stained with gel red. The amplicons were purified using the GeneJet purification kit according to the manufacturer's instructions (Thermofisher Scientific). The termination cycle sequencing reaction was carried out using the BigDye terminator V3.1 cycle sequencing kit (Thermofisher Scientific), and amplification primers were also used in sequencing. Post termination reaction, the products were purified then dissolved in HI DI formamide (Thermofisher Scientific) and loaded on a 3130xl genetic analyser. Base calling was performed using the sequencing software v5.1. Assembly and analysis were carried out using Sequencher v5.0 and genotypes were determined using Basic Local Alignment Search Tool (BLAST) on the National Centre for Biotechnology Information (NCBI) and also Bacterial and Viral Bioinformatics Resource Centre (BV-BRC).

3.5.3 Whole genome amplification

The Qiagen one step RT-PCR kit was used to synthesise the complementary DNA (cDNA) with further amplification according to previous protocol (73). The 5 µl of extracted RNA as well as the RV gene specific primers from previous published methods (73,74) were incubated at 95°C for five minutes. Thereafter, reverse transcription reaction occurred at 45°C for 30 minutes, with subsequent 40 cycles with the following thermocycling conditions:

- 94°C for 10 seconds.
- Annealing at 55°C for 1 minute.
- Extension at 68°C for 3 minutes.
- Final extension at 68°Cfor 10 minutes.

The PCR products were visualised on a 1% agarose gel stained with gel red (Biotium). Post amplification products were purified using the GeneJet PCR purification kit (Thermofisher Scientific) as per manufacturer protocol.

3.5.4 Amplicon purification

The PCR products were purified using the GeneJet PCR purification kit (Thermofisher Scientific) according to the manufacturer's instruction. Briefly, the sample and binding buffer were mixed 1:1 then transferred to the spin column, which was centrifuged at 14 500 rpm for 60 seconds. This was followed by the addition of 700 µL wash buffer, which was further centrifugation at 14 500 rpm for 60 seconds and finally dry spunned and 50 µL elution of the DNA using the elution buffer.

3.5.5 Nucleic quantification

The amplicons were quantified using the Qubit 3 fluorometer (Invitrogen). The working reagent solution was prepared by mixing 1 µL of Qubit reagent with 199 µl Qubit buffer in order to have the dilution of 1:200. Further, the two standard calibrators were prepared by pipetting 10 µL of standard to 190 µL of prepared working solution then used to calibrate the Qubit 3 fluorometer. Samples were prepared by pipetting 199 µL of working solution into a 0.5 mL tube, then 1 µL of sample was added and incubated at room temperature for 2 minutes. The quantified DNA for each of the 11 RV genes ranged from (3 ng/µL-9.19 ng/µL).

3.5.6 DNA library preparation

The library preparation was performed according to the Illumina DNA Prep protocol (Illumina) (75). Briefly, the quantified DNA was first normalised then transferred to initiate the first step of library preparation, called tagmentation. The tagmentation process involved Bead-linked transposome technology (BLT) which fragmented and tagged the DNA with adapter sequences. The tagmentation mixture was performed by adding 30 µL of DNA to 20 µL of the tagmentation reagents. The mixture was incubated on a thermocycler for 15 minutes at 55°C with a subsequent hold step at 10°C. The second step was clean up of tagmentation products which involved washing the adapter tagged DNA and stopping the tagmentation reaction by addition of 10 µL stop tagmentation buffer with further incubation at 37°C for 15 minutes. The plate was then placed on the magnetic stand for 3 minutes, and whilst on the magnetic stand the supernatant was removed and discarded. The plate was removed from the magnetic stand, then 100 µL of tagment wash buffer was added directly on the beads. Full resuspension of the beads was achieved by slowly pipetting up and down, with subsequent return of the plate on the magnetic stand. The next stage involved amplification of tagmented DNA by addition of the index (i7), index (i5) and oligos required for the cluster generation Sequencing primer 1, Sequencing primer 2 as well as additional of the enhanced PCR mix reagent. The amplification mixture was transferred to the thermocycler for amplification. Thermocycling conditions are presented in Table 2.

Table 2*:* **DNA Thermocycling steps**

Step	Time	Temperature	Cycle
Heating	3 minutes	68°C	1
Initial denaturation	3 minutes	98°C	1
Denaturation	45 seconds	98°C	6
Annealing	30 seconds	62°C	
Extension	2 minutes	68°C	
Final extension	1 minutes	68°C	1
Hold		10°C	1

3.5.7 Purification of DNA library

This step used the double-sided bead purification process to purify amplified tagged DNA. The 96 well plate containing the library was placed on the magnetic stand for 5 minutes, followed by transferring 45 µL of supernatant to the new 96 well plate. Then 85 µL mixture containing nuclease free water and Illumina Purification Beads (IPB), was added to each well containing the supernatant. The mixture was performed by slowly pipetting 10 times followed by incubation of the plate at room temperature for 5 minutes. Post incubation, the plate was placed on the magnetic stand for 5 minutes. Thereafter, 125 µL supernatant was transferred to the new plate with 81 µL of IPB, and subsequently mixed by slowly pipetting up and down 10 times. The mixture was incubated for 5minute at room temperature, followed by placing the 96 well plate on the magnet. The supernatant was removed and discarded. While the plate was on the magnet, the library was washed twice by addition of 100 µL of freshly prepared 80% ethanol without mixing, for 30 seconds with subsequent removal and discarding of ethanol. The last stage was elution of the DNA from the beads carried out by addition of 32 µL of resuspension buffer to beads with subsequent incubation on the magnetic stand for 2 minutes. Finally, 30 µL of elute was pipetted into 1.5mL tubes. The library was quantified then normalised with subsequent pooling of the libraries. The pooled library was denatured by addition of 1N of freshly prepared sodium hydroxide (NaOH). The denatured library was diluted to a 20 pM loading concentration with addition of HT1. Then 600 µL of the 20 pM was loaded on the 500 cycle sequencing cartridge.

3.6 Bioinformatics

3.6.1 Genome assembly

Post sequencing from the Illumina Miseq, paired end reads were imported to the Geneious Prime software version 2023.04. The FASTQ files were first trimmed by using the BBDuk (Bestus Bioinformaticus Decontamination using Kmers), a plugin in the Geneious prime software(76). The trimmed sequence reads were assembled using both the *de novo* as well as mapped to reference sequences (72). Lastly, the consensus sequence was extracted and used for the downstream analysis.

3.6.2 Determination of genotype

The genotype for each of the 11 segments of the genome was determined by utilising the Bacterial and Viral Bioinformatics Resource Centre (BV-BRC), an online database which house the ViPR (77). Additionally, an online database was used as compensatory method in the genotype identification for each segment of the genome, the Basic Local Alignment Search Tool (BLAST) on the National Centre for Biotechnology Information (NCBI) (78).

3.6.3 Phylogenetic analysis

For each of the 11 segments of the RV genome, multiple reference sequences were obtained from both the NCBI using BLAST, as well as BV-BRC database. The selection of reference sequences was based on the following. Firstly, historical strain with complete ORF of the gene applied in the designation of lineages, for instance strain Wa, DS-1 and L26 secondly, sequences from vaccine strain and lastly closely related strains with complete ORF of the gene from Sub Saharan Africa.

The multiple sequence alignment was performed using MAFFT, a plugin in the Geneious software, as well as MUSCLE in MEGA V6 (76,79). The maximum likelihood trees for each of the 11 segments of the genome were constructed based on generated substitution models in the MEGA v6. The model with the lowest BIC (Bayesian Information Criterion) value was selected for the phylogenetic tree construction (80,81). The models used to build the phylogenetic trees in this study were: T92+G (VP1, VP2, VP3, VP4, VP7, NSP4 and NSP5), T92+G+I (NSP1, NSP2, NSP3 and VP6).

3.7 Ethical statement

Ethical approval was obtained from the University of Zambia Biomedical Research Ethics Committee (UNZABREC) for this study (UNZABREC Ref# 3569-2022) and for the parent RV trial (UNZABREC Ref# 003-02-18) (Addendum A). Informed written consent was obtained from mothers or guardians of the children included in this study.

CHAPTER 4: RESULTS

4.1 Baseline characteristics as well as genotyping of VP4 and VP7

As shown in Table 3, the three RV infections from participant infants RV2088, RV2106 and RV2150 were identified as G1P[4], G12P[4] and G12P[8] genotypes respectively using the sanger sequencing. Children among which these infections occurred had a mean age of 22.3 months, two out of three were male and only one was HIV exposed born from HIV positive mother. Two infants had received three doses of Rotarix vaccine, and one had received two doses. Based on RV-IgA titre results at between baseline and one month after second dose Rotarix, two infants had seroconverted (RV2088 and RV2150) and one had not seroconverted (RV2106).

Table 3*:* **Infant baseline factors and immune characteristics**

ID	RV2088	RV2106	RV2150
Genotype	G1P[4]	G12P[4]	G12P[8]
Age(Months)	22	22	23
Sex	male	female	male
HIV exposure	unexposed	exposed	unexposed
Seroconversion	yes	no	yes

4.2 Whole genome genotype constellation

Using the RCWG classification, we detected a mono reassortant strain for RV2088 denoted as RVA/Human-wt/ZMB/CIDRZ-RV2088/2020/**G1**P[4]-I2-R2-C2-M2-A2-N2-T2-E2-H2 and a multiple reassortant strain for RV2106 denoted as RVA/Human-wt/ZMB/CIDRZ-RV2106/2020/**G12**P[4]-**I1**-R2-C2-M2-A2-**N1**-T2-**E1**-H2. The two reassortants had mostly the DS-1-like genetic backbone with Wa-like characteristics (exchanged genes bolded). A typical Wa-like strain was detected for RV2150 denoted as RVA/Human-wt/ZMB/CIDRZ-RV2150/2020/G12P[8]-I1-R1-C1-M1-A1-N1-T1-E1-H1. For each of the 11 segments of the genome of the study strains complete or near complete lengths of the ORFs were obtained (Table 4). The open reading frames of sequences for all the 11 genes of the breakthrough strains were deposited in the GenBank under the accession numbers (OR338245-OR338277)

Table 4: Whole genome genotype constellation of rotavirus strains responsible for breakthrough infections

Strain ID		VP7	VP4	VP6	VP1	VP2	VP3	NSP1	NSP2	NSP3	NSP4	NSP5
CIDRZ-RV2088	Genotype constellation	G1	P[4]	I2	R2	C2	M2	A2	N2	T2	E2	H2
	Open Reading frame length	981	2359	1194	3267	2658	2520	1349	954	933	528	603
	Reads mapped to contig	10,387	43,705	11,234	55,613	94,857	61,850	5,640	90,290	12,856	8,750	9,140
CIDRZ-RV2106	Genotype constellation	G12	P[4]	I1	R2	C2	M2	A2	N1	T2	E1	H2
	Open Reading frame length	981	2359	1194	3267	2658	2520	1349	954	933	528	603
	Reads mapped to contig	62,513	157,158	45,271	147,115	73,591	87,521	14,769	58,744	23,951	29,568	35,281
CIDRZ-RV2150	Genotype constellation	G12	P[8]	I1	R1	C1	M1	A1	N1	T1	E1	H1
	Open Reading frame length	981	2359	1194	3267	2658	2520	1349	954	933	528	603
	Reads mapped to contig	5,438	92,617	12,771	21,755	31,461	42,856	7,301	88,371	15,846	183,160	31,793

The Orange accent color represented the Wa-like genogroup, whilst the green represented the DS-1 like genogroup

4.3 VP7 Phylogenetic analysis

In order to comprehend the relationship between the breakthrough and global strains, a phylogenetic tree was constructed for the VP7 gene of RV. The G1 breakthrough strain clustered in lineage II along with Rotarix vaccine, as well as the designated lineage II reference strains (18,72,82) (Figure 5). The breakthrough strain CIDRZ-RV2088/2020/G1P[4] shared 99.7% nucleotide identity with the Rotarix vaccine, as well as vaccine derived strains from Japan (KY616899.1), Belgium (ON855136.1) and the USA (MF469224.1). Furthermore, the phylogenetic tree analysis has shown the two G12 strains clustered in lineage III, which comprised of strains from Africa, USA and Asia (83,84). The two G12 strains exhibited 98% to 99.08% nucleotide identity with strains from Mozambique (MG926719.1), Rwanda (MT163190.1), South Africa (KJ752819.1) and Nepal (LC374137.1). The G12 strains (CIDRZ-RV2150 G12P[4] and CIDRZ-RV2106G12P[8]) shared the nucleotide identity of 100% (Addendum B).

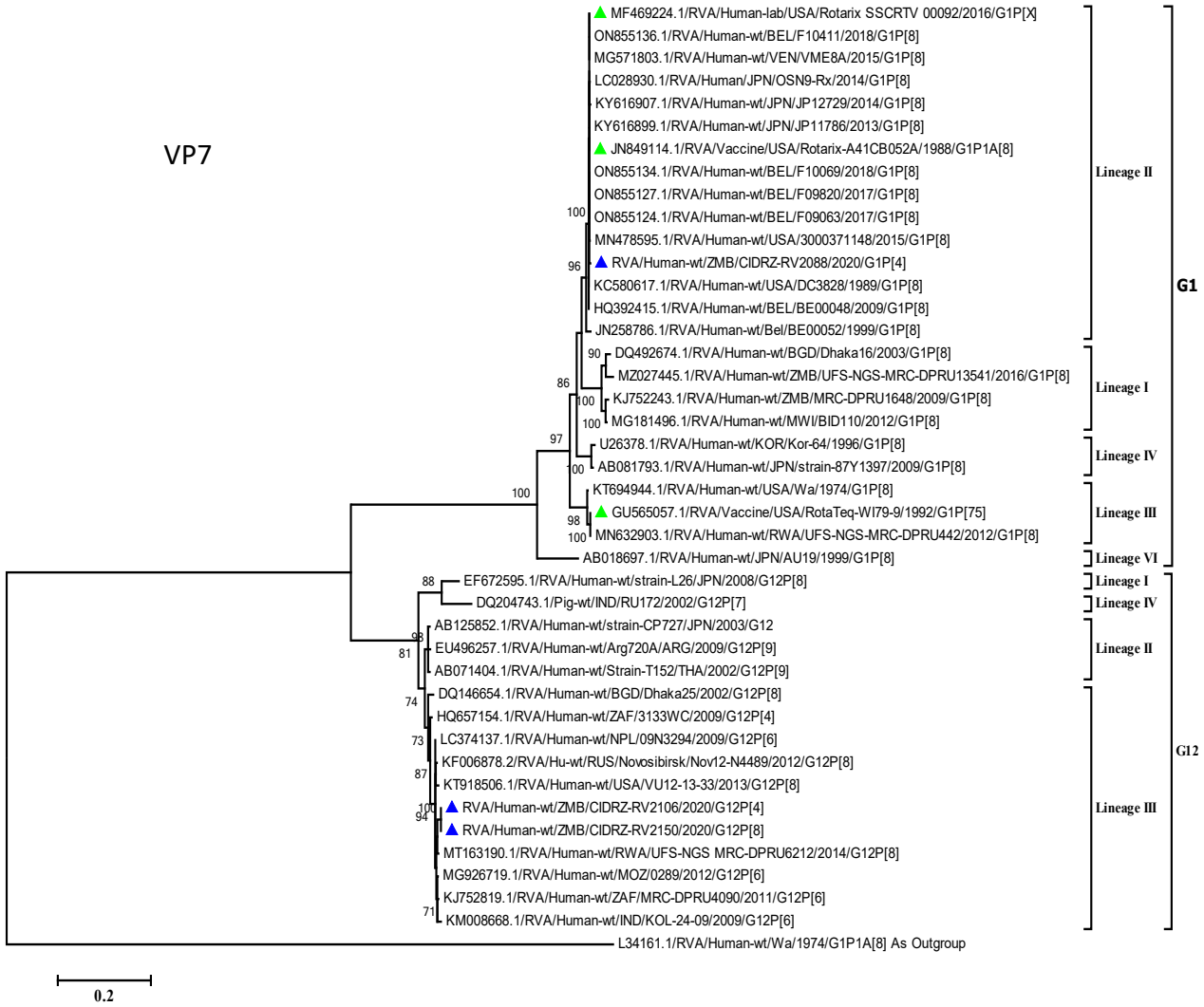

Figure 5: Maximum likelihood phylogenetic tree between the VP7 gene of the Breakthrough G1 and G12 strains as well as global strains. Green filled triangles represented vaccine sequences, whilst Breakthrough strains blue filled triangles. Scale at the bottom indicated nucleotide substitutions per site, whilst bootstrap values greater than or equal to 70 were shown on the branches.

4.4 Comparative analysis of VP7 antigenic epitope between the vaccines and breakthrough strains

The VP7 forms part of the outer protein capsid, involved in eliciting of the neutralising antibodies (85). The VP7 antigenic epitope comprised of two domains, the 7-1 and 7-2. The 7-1 is further subdivided into 7-1a and 7-1b. The VP7 antigenic epitope composed of 29 amino acids (85). The breakthrough strain CIDRZ-RV2088/2020/G1P[4] shared all the 29 amino acids residues as the Rotarix vaccine as shown in Table 5. Analysis of the antigenic epitope of strains (CIDRZ-

RV2150/2020/G12P[4] and CIDRZ-RV2106/2020/G12P[8]) revealed 12 conserved amino acids out of 29 in comparison to the Rotarix vaccine. The G12 strains exhibited eight amino acid differences in the 7-1a (T87S; N94T; G96P; E97D; K99T; D100N; S123D and V125S), whereas in 7-1b three amino acid differences were observed (N211D; D213T and T242N). Furthermore, six amino acids differences were observed in the 7-2 (K143Q; D145Q; Q146N; N147S; M217E and N221A).

Table 5: Amino acids alignment of VP7 antigenic sites between breakthrough strains and Rotarix

Differences in composition of amino acids in antigenic sites of VP7 Protein between breakthrough strains and rotarix vaccine

		7-1a													7-1b						7_2									
	Lineage	87	91	94	96	97	98	99	100	104	123	125	129	130	291	201	211	212	213	238	242	143	145	146	147	148	190	217	221	264
JN849114/Rotarix vaccine	II	T	T	N	G	E	W	K	D	Q	S	V	V	D	K	Q	N	V	D	N	T	K	D	Q	N	L	S	M	N	G
ZMB/CIDRZ-RV2088/2020/G1P[4]	II	.	.	.	.	.	.	.	.	.	.	.	.	.	.	.	.	.	.	.	.	.	.	.	.	.	.	.	.	.
ZMB/CIDRZ-RV2150/2020/G12P[8]	III	S	.	T	P	D	.	T	N	.	D	S	.	.	.	.	D	.	T	.	N	Q	Q	N	S	.	.	E	A	.
ZMB/CIDRZ-RV2106/2020/G12P[4]	III	S	.	T	P	D	.	T	N	.	D	S	.	.	.	.	D	.	T	.	N	Q	Q	N	S	.	.	E	A	.
MK059434/DPRU4165/2010/G12P[6	III	S	.	T	P	D	.	T	S	.	D	S	.	.	.	.	D	.	T	.	N	Q	Q	N	S	.	.	E	A	.
MK059426/DPRU1765/2012/G12P[6	III	S	.	T	P	D	.	T	N	.	D	S	.	.	.	.	D	.	T	.	N	Q	Q	N	S	.	.	E	A	.
MK059427/DPRU2495/2011/G12P[6	III	S	.	T	P	D	.	T	N	.	D	S	.	.	.	.	D	.	T	.	N	Q	Q	N	S	.	.	E	A	.
MZ027445/DPRU3541/2016/G1P[8]	I	.	.	S	.	.	.	.	.	.	N	.	.	.	R	.	.	.	.	.	.	.	.	.	.	.	.	T	.	.
MZ027423/DPRU3232/2016/G1P[8]	I	.	.	S	.	.	.	.	.	.	N	.	.	.	R	.	.	.	.	.	.	.	.	.	.	.	.	T	.	.
KJ752243/DPRU1648/2009/G1P[8]	I	.	.	.	.	.	.	.	.	.	N	.	.	.	R	.	.	.	.	.	.	.	.	.	.	.	.	T	.	.

Amino acid alignment of the antigenic sites of the G1 and G12 strains highlighted black, reference strains green and red Rotarix vaccine. Filled blue triangles represented amino residues positions that have been shown to escape neutralization with monoclonal antibodies. Dot represented conserved amino acids.

4.5 Phylogenetic analysis of VP4 gene

To determine the relationship of the VP4 gene study strains, a phylogenetic tree was built which contained global strains from previous published studies (72,86,87). The P[4] strains (CIDRZ-RV2088/2020/G1P[4] and CIDRZ-RV2106/2020/G12P[4]) belonged to lineage IV along with strains from Malawi, Uganda, Pakistan and Thailand (Figure 6). The P[4] breakthrough strains displayed nucleotide identities of 99 % with strains from Malawi (ON792094.1, ON792083.1) and Pakistan (MH182440.1) (Addendum B). Furthermore, the strains shared nucleotide identities of 99.8% between them. On the other hand, strain CIDRZ-RV2106/2020/G12P[8] belonged to lineage III together with strains from Africa, the USA and Europe. The P[8] strain shared 99% nucleotide identities with human RV strains from Mozambique (MT737518.1,MT737519.1) and the USA (KT919340.1) (Addendum B). The P[8] strain further shared 90% nucleotide identity with the P[8] Rotarix vaccine.

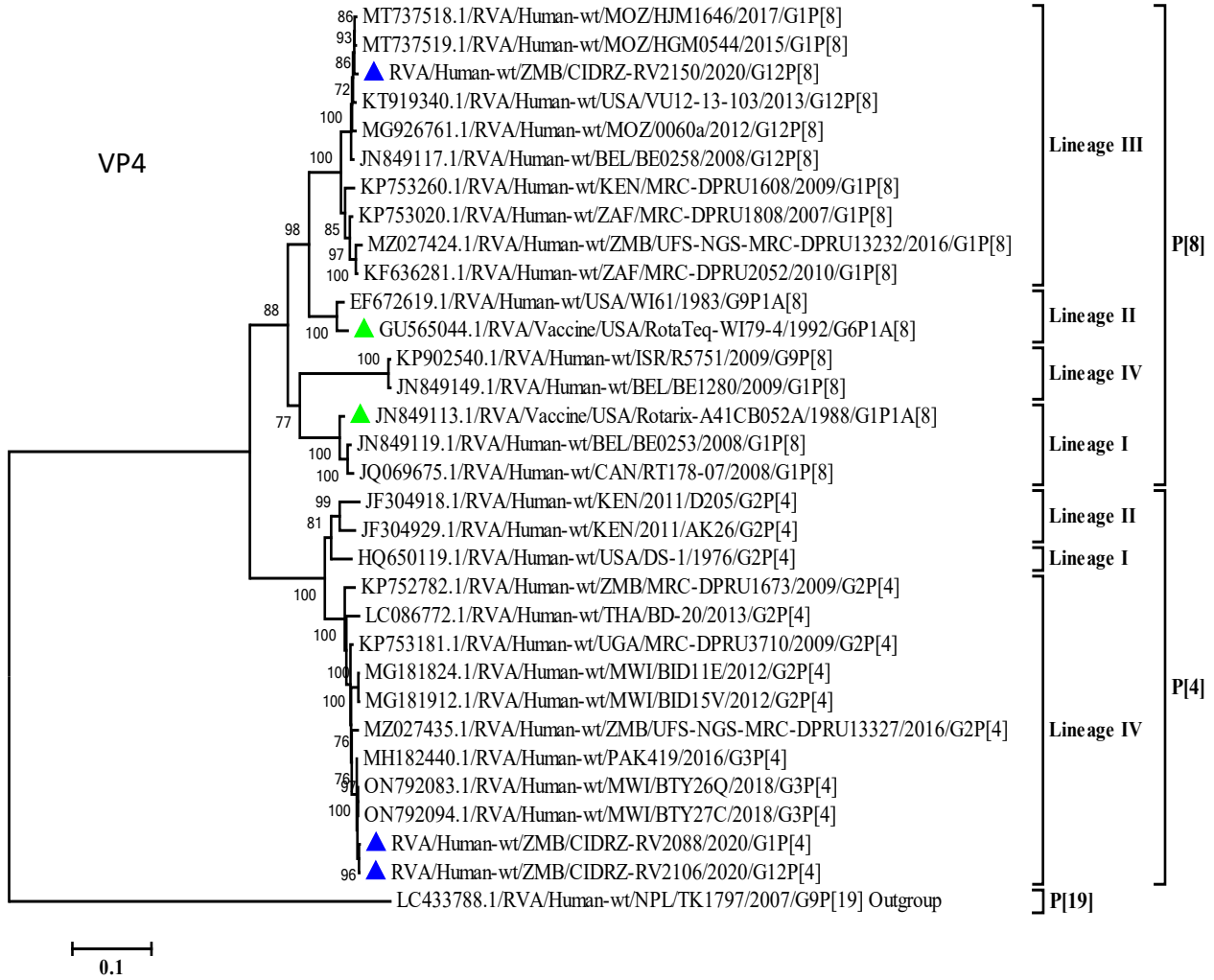

Figure 6: Maximum likelihood phylogenetic tree between the VP4 gene of the Breakthrough P[8] and P[4] strains as well as global strains. Green filled triangles represented vaccine sequences whereas blue filled triangles represented breakthrough strains. Scale at indicated nucleotide substitutions per site, whilst bootstrap values greater than or equal to 70 were shown on the branches.

4.6 Comparative analysis of VP4 neutralising antigenic epitope between Rotarix vaccine and breakthrough strains

The VP4 spike protein is proteolytically cleaved into the two distinctly functional proteins of the VP5* and VP8* (72). The VP8 epitope is composed of four subdomains, 8-1, 8-2, 8-3 and 8-4, while the VP5 is comprised of five subdomains, 5-1, 5-2, 5-3, 5-4 and 5-5 (72). The combination of antigenic epitopes of VP8 and VP5 is composed of 37 amino acids. In the present study we report 25 conserved amino acids out of 37 in all breakthrough strains in comparison to the Rotarix vaccine (Table 6). The breakthrough strains with P[4] genotype had one amino acid difference in the 8-1; (E150D) further

in subdomain 8-2 all the amino acids were conserved, in subdomain 8-3 there were eight observed amino acid differences (N113S, P114Q, V115T, D116N, S125N, S131E, D133S and N135D). Lastly, in subdomain 8-4 only one amino acid difference was observed (N89D). The VP5 subunit of spike protein comprised of five subdomains with the composition of 12 amino acids, of which only one amino acid difference (I388L) was observed. The comparison of P[8] breakthrough strain with Rotarix vaccine revealed two amino acid substitutions in the 8-1 subdomain (E150D and N195G). In the 8-3 subdomain three amino acid substitutions were observed (S125N, S131R and N135D). Finally, in the VP8* subdomain 8-4 all the amino acids were conserved. The VP5* subunit of the spike protein of the breakthrough strain P[8] had shown all amino acids conserved.

Table 6: Amino acid alignment of the antigenic sites of the VP4 between Rotarix vaccine and breakthrough strains

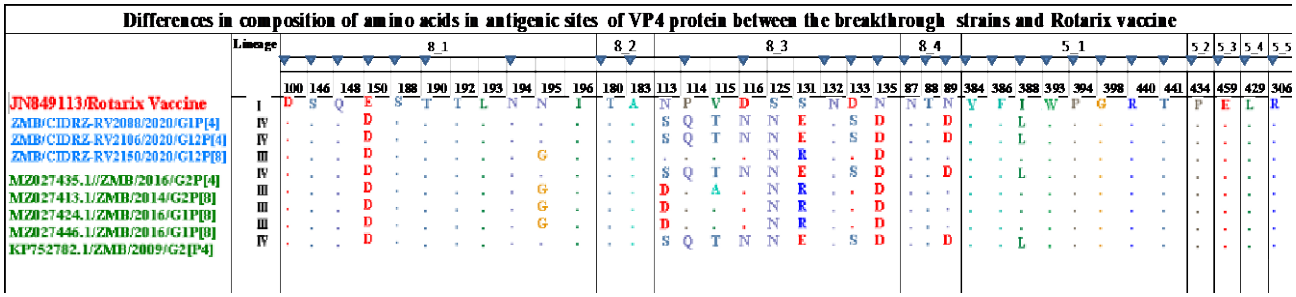

Amino acid alignment of the antigenic sites of the Rotarix vaccine is highlighted in red while P[4] and P[8] breakthrough strains are highlighted blue and reference strains. Filled blue triangles represented amino residues that have been shown to escape neutralisation with monoclonal antibodies. Dot represented conserved amino acids.

4.7 Phylogenetic analysis of VP1

The VP1 gene revealed that the Wa-like strain CIDRZ-RV2150/2020/G12P[8] belonged to lineage R1 along with strains from South Africa, Mozambique, Kenya, Belgium and Asia (Figure 7). The Wa-like Zambian strain displayed 98% homology with strains from South Africa (KJ752339.1), Malawi (MG181480.1) and Bangladesh (DQ146649.1). Furthermore, the two DS-1-like strains, CIDRZ-RV2088/2020/G1P[4] and CIDRZ-RV2106/2020/G12P[4], clustered in lineage R2 together with a Zambian strain from 2015. The two DS-1-like strains shared 98-99% nucleotide identity along with the 2015 Zambian strain (OQ133150.1), as well as strains from Malawi (ON792025.1) and Pakistan (MH166402.1).

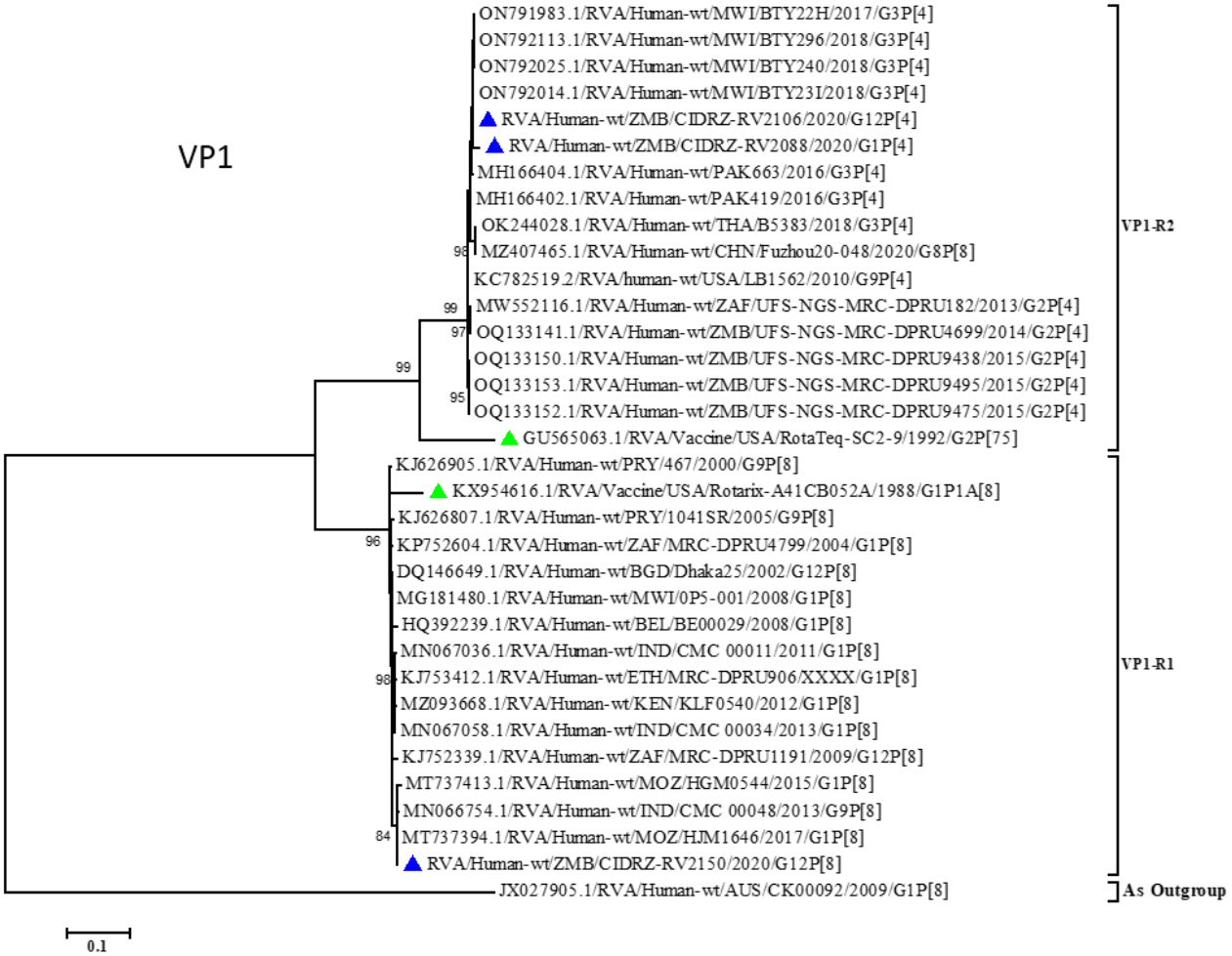

Figure 7: Maximum likelihood phylogenetic tree between the VP1 gene of the breakthrough strains as well as global strains. Green filled triangles represented vaccine sequences whereas Blue filled triangles Breakthrough strains. Scale at the bottom indicated nucleotide substitutions per site, whilst bootstrap values greater than or equal to 70 were shown on the branches.

4.8 Phylogenetic analysis of VP2

Phylogenetic analysis of the VP2 gene revealed that the Wa-like strain CIDRZ-RV2150/2020/G12P[8] belonged to lineage C1, along with strains from South Africa, Mozambique, Kenya, the USA and Asia (Figure 8). The Wa-like Zambian strain shared nucleotide identity of 98-99% with strains from Mozambique (MT737433.1), Italy (KU048553.1), Rwanda (MN633028.1) and South Africa (MT855252.1). The DS-1 like strains CIDRZ-RV2088/2020/G1P[4] and CIDRZ-RV2106/2020/G12P[4]) belonged to lineage C2 and shared 98-99% nucleotide homology with strains from Malawi (ON792114.1) and Pakistan (MH166409.1).

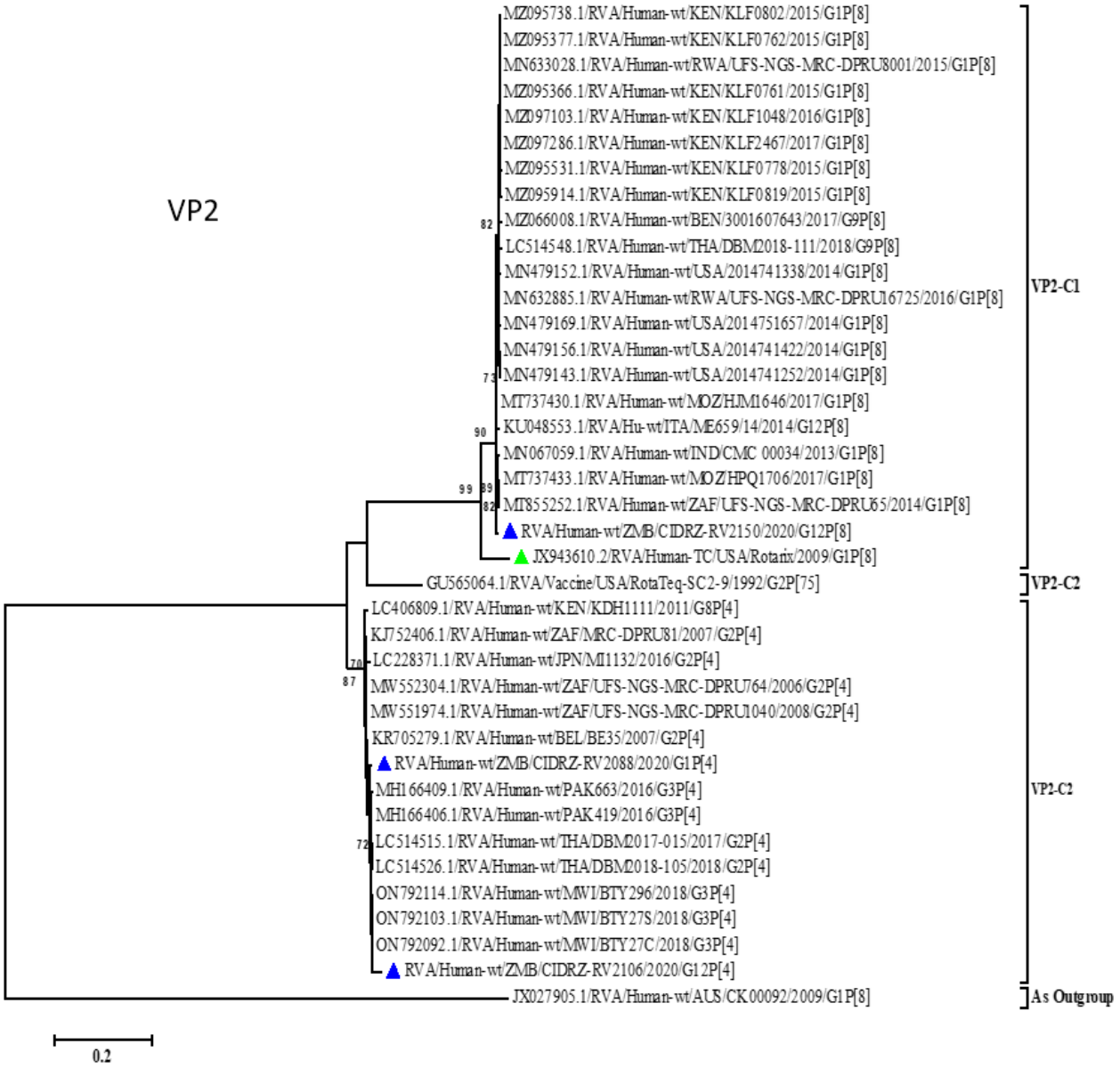

Figure 8: Maximum likelihood phylogenetic tree between the VP2 gene of the breakthrough strains as well as global strains. Green filled triangles represented vaccine sequences whereas Blue filled triangles Breakthrough strains. Scale at the bottom indicated nucleotide substitutions per site, whilst bootstrap values greater than or equal to 70 were shown on the branches.

4.9 Phylogenetic analysis of VP3

The VP3 segment of the Wa-like breakthrough strain CIDRZ-RV2150/2020/G12P[8] phylogenetically belonged to lineage M1 together with strains from India, Europe and the USA (Figure 9). The Wa-like strain shared the 99% nucleotide identity with strains from Mozambique (MT737465.1), India (MN066756.1) and Italy (KU048583.1), whereas the DS-1-like strain clustered in lineage CIDRZ-

RV2088/2020/G1P[4] and CIDRZ-RV2106/2020/G12P[4], M2 along with strains from Malawi, Pakistan, India and the USA with shared nucleotide identities ranging from 98%-99%.

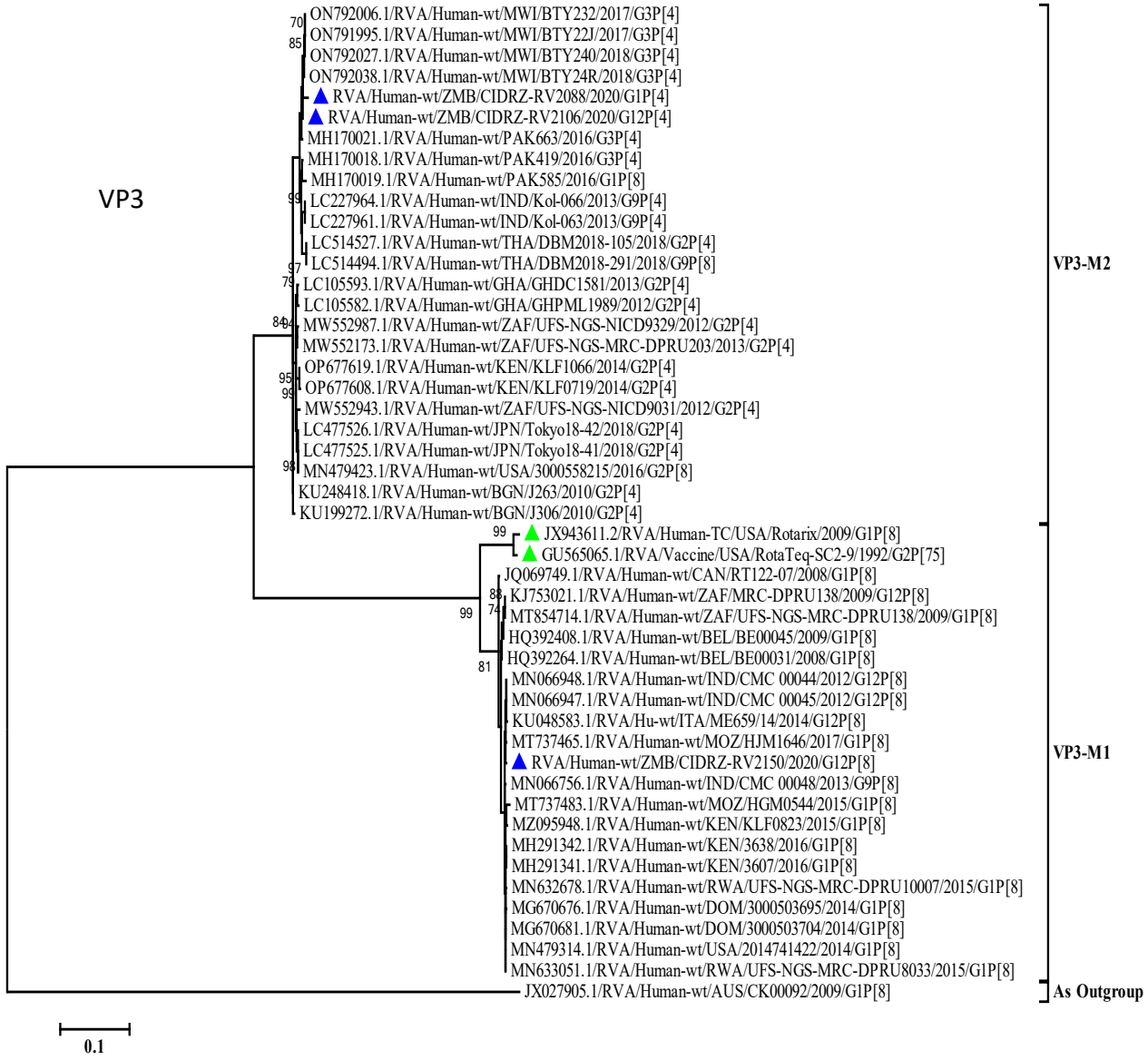

Figure 9: Maximum likelihood phylogenetic tree between the VP3 gene of the breakthrough strains as well as global strains. Green filled triangles represented vaccine sequences whereas Blue filled triangles indicated Breakthrough strains. Scale at the bottom indicated nucleotide substitutions per site, whilst bootstrap values greater than or equal to 70 were shown on the branches.

4.10 Phylogenetic analysis of VP6

Phylogenetic analysis of the VP6 gene has shown strains CIDRZ-RV2106/2020/G12P[4] and CIDRZ-RV2088/2020/G1P[4] clustering in lineage I2 along with strains from Asia and Africa, although strain

CIDRZ-RV2106/2020/G12P[4] clustered separately from the other strains (Figure 10). This strain shared the highest nucleotide identity of 91.8% with strain from Rwanda (gb;MT163203), whereas strain (CIDRZ-RV2088/2020/G1P[4]) displayed the highest nucleotide identity of 97.9 % with strain from Malawi (ON791997.1), Pakistan(MH170023.1) and Russia (KC713896.1). Furthermore, the Wa-like strain CIDRZ-RV2150/2020/G12P[8] belonged to the I1 lineage and shared 99% nucleotide similarities with strains from Mozambique(MT737536.1) and India (MN067062.1) .

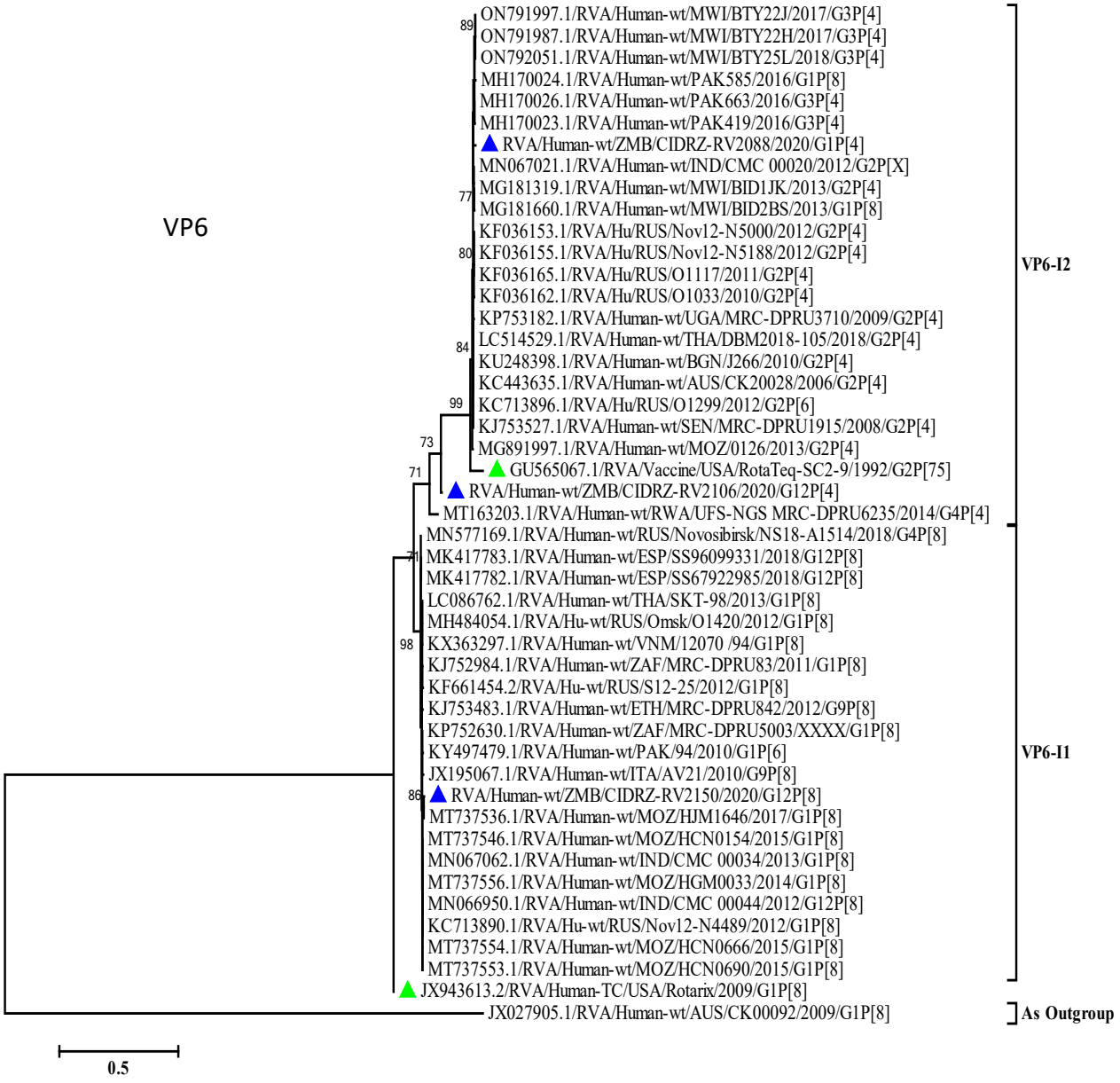

Figure 10: Maximum likelihood phylogenetic tree between the VP6 gene of the breakthrough strains as well as global strains. Green filled triangles represented vaccine sequences whereas Blue filled triangles indicated Breakthrough strains. Scale at the bottom indicated nucleotide substitutions per site, whilst bootstrap values greater than or equal to 70 were shown on the branches.

4.11 Phylogenetic analysis of NSP1

The Wa-like strain CIDRZ-RV2150/2020/G12P[8] belonged to lineage A1 along with strains from Eastern and Southern Africa, as well as strains from Nepal and the USA (Figure 11). The Wa-like study strain shared 99% nucleotide identity with strains from Mozambique (MT737605.1), Kenya (MZ097119.1), South Africa (MT854759.1) and Nepal (LC374132.1). On the other hand, the DS-1-like strains CIDRZ-RV2088/2020/G1P[4] and CIDRZ-RV2106/2020/G12P[4]) belonged to the lineage A2 and exhibited highest 97% nucleotide identity with human RV strains from Malawi (ON792097.1, ON792020.1 and ON791988.1).

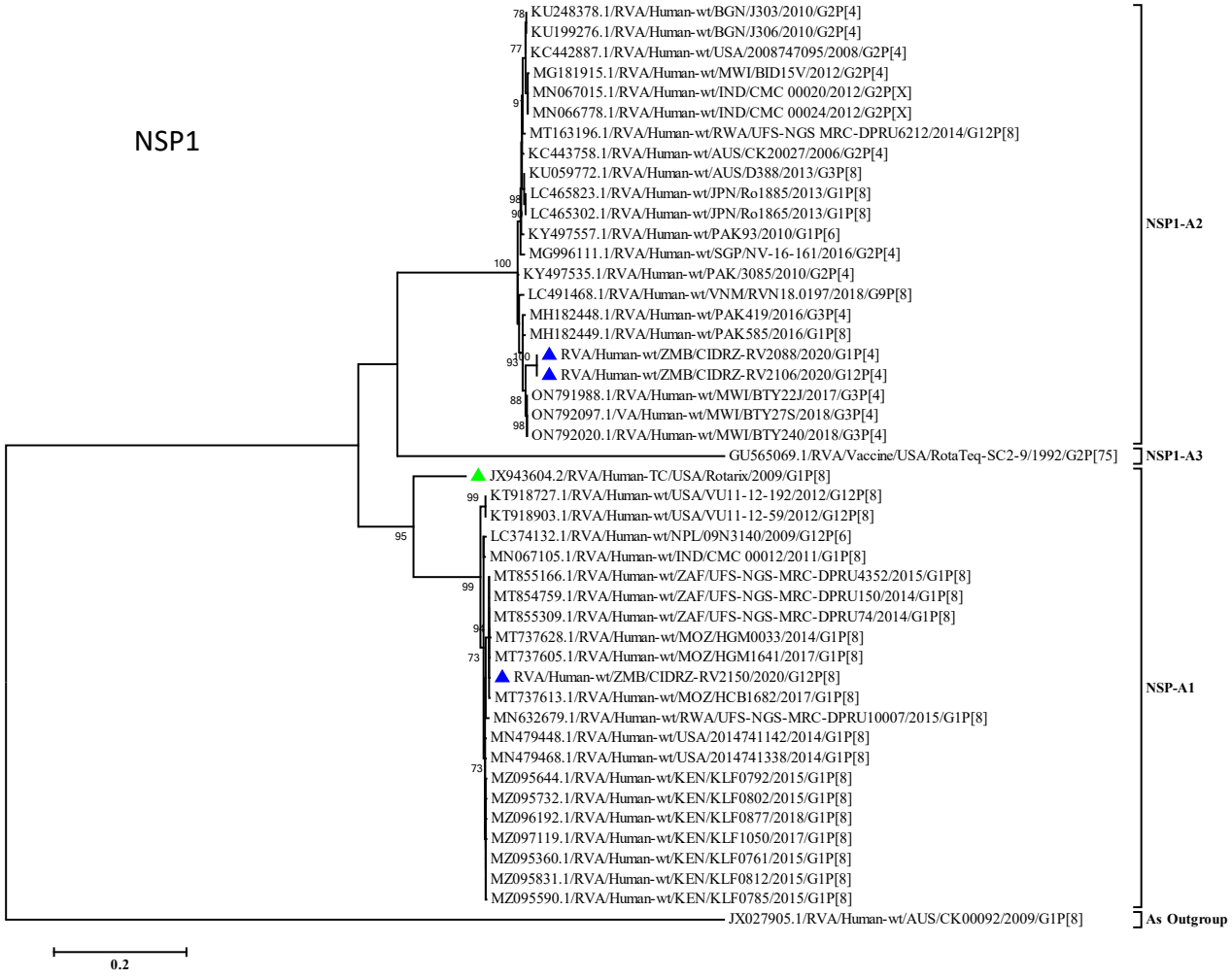

Figure 11: Maximum likelihood phylogenetic tree between the NSP1 gene of the breakthrough strains as well as global strains. Green filled triangles represented vaccine sequences whereas Blue filled triangles indicated Breakthrough strains. Scale at the bottom indicated nucleotide substitutions per site, whilst bootstrap values greater than or equal to 70 were shown on the branches.

4.12 Phylogenetic analysis of NSP2

Phylogenetic analysis of the NSP2 gene of CIDRZ-RV2150/2020/G12P[8] strain revealed the Wa-like study strain belonged to lineage N1 along with strains from Mozambique, Malawi, Kenya, Japan and India, with the highest shared nucleotide identity of 99.3% with a strain from Mozambique (MT737644.1), whereas the DS-1-like study strains CIDRZ-RV2088/2020/G1P[4] and CIDRZ-RV2106/2020/G12P[4] clustered in lineage N2. Furthermore, strain CIDRZ-RV2106/2020/G12P[4] clustered separately in lineage N2 and showed the highest nucleotide identity of 94% with strains from Malawi (ON792109.1, ON792087.1) and Pakistan (MH182456.1) (Figure 12).

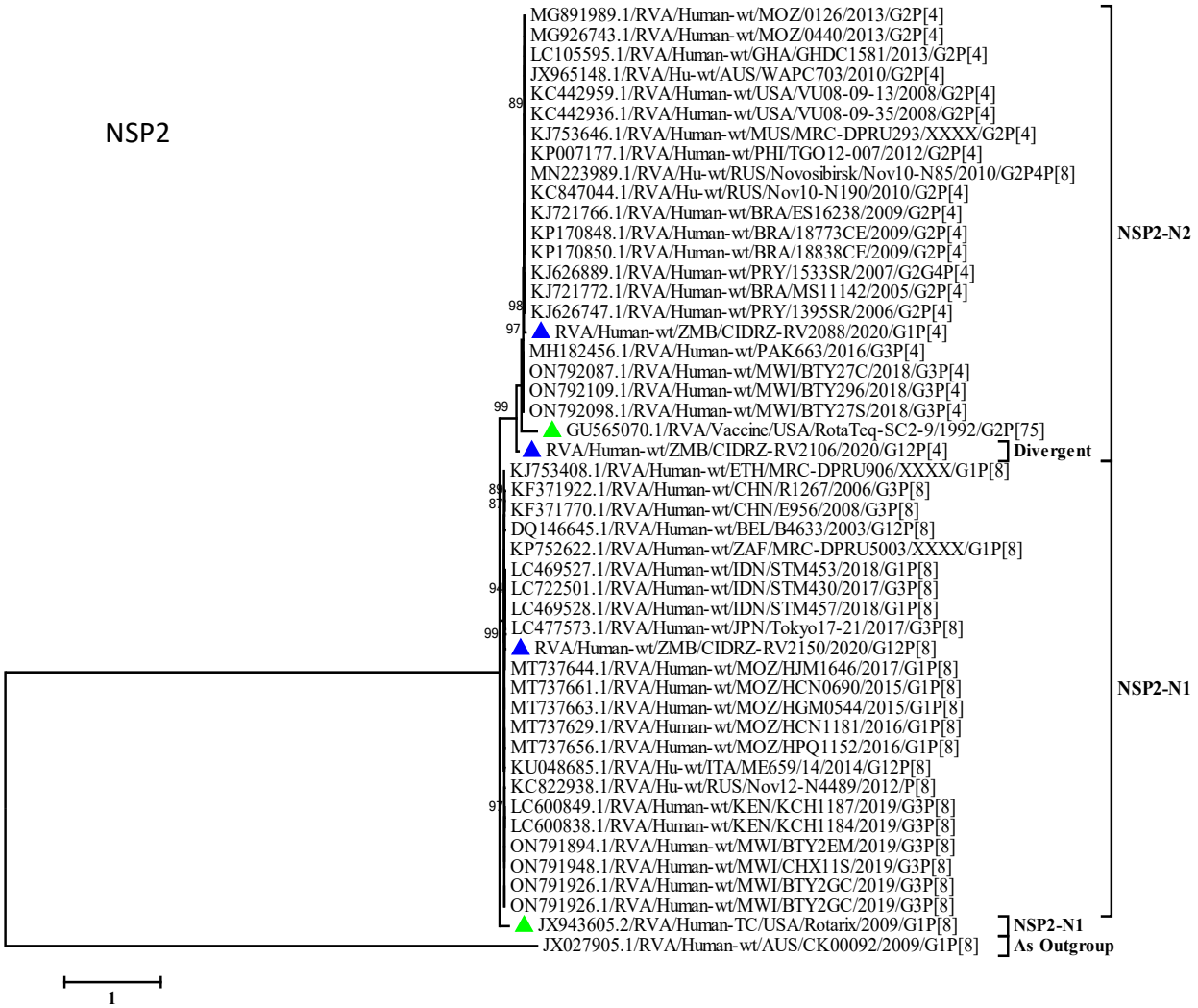

Figure 12: Maximum likelihood phylogenetic tree between the NSP2 gene of the breakthrough strains as well as global strains. Green filled triangles represented vaccine sequences whereas Blue filled triangles indicated Breakthrough strains. Scale at the bottom indicated nucleotide substitutions per site, whilst bootstrap values greater than or equal to 70 were shown on the branches.

4.13 Phylogenetic analysis of NSP3

The Wa-like strain CIDRZ-RV2150/2020/G12P[8] belonged to lineage T1 and shared highest nucleotide homology of 99% with strains from Mozambique (MT737680.1 and MT737699.1). Furthermore, the DS-1-like strains CIDRZ-RV2088/2020/G1P[4] and CIDRZ-RV2106/2020/G12P[4] clustered in lineage T2 along with strains from Malawi, Pakistan and the USA. In addition, strain CIDRZ-RV2106/2020/G12P[4] was separately grouped in lineage T2 and shared the maximum nucleotide identity of 91% with strains from Malawi (ON792110.1, ON792099.1) and Pakistan (MH182461.1) (Figure 13).

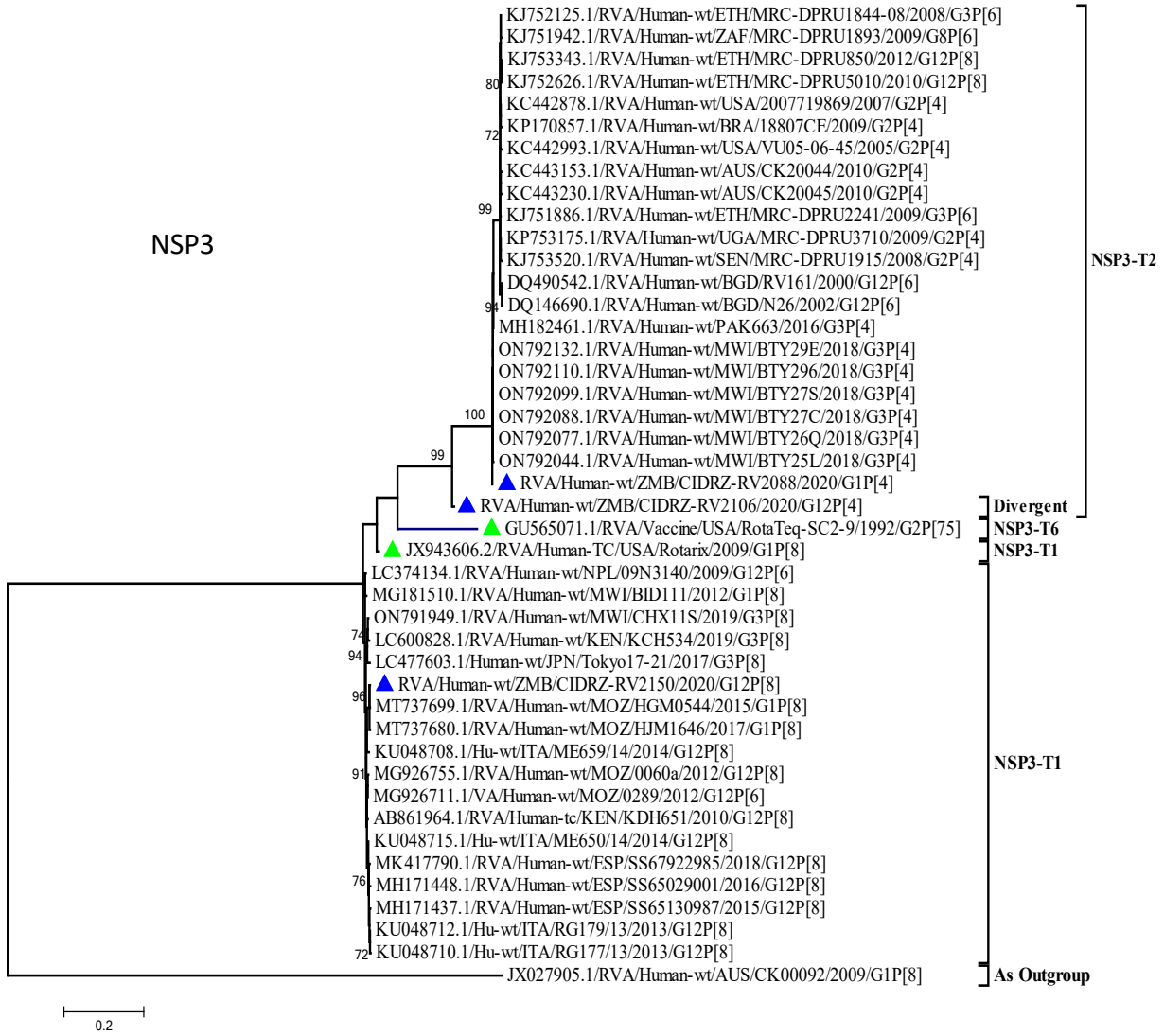

Figure 13: Maximum likelihood phylogenetic tree between the NSP3 gene of the breakthrough strains as well as global strains. Green filled triangles represented vaccine sequences whereas Blue filled triangles indicated Breakthrough strains. Scale at the bottom indicated nucleotide substitutions per site, whilst bootstrap values greater than or equal to 70 were shown on the branches.

4.14 Phylogenetic analysis of NSP4

The Phylogenetic analysis of NSP4 gene has shown the study strains (CIDRZ-RV2106/2020/G12P[4] and CIDRZ-RV2150/2020/G12P[8]) clustered in lineage E1, along with strains from Africa, Asia and Brazil. Furthermore, strain CIDRZ-RV2106/2020/G12P[4] clustered separately in the lineage E1 from other strains. It shared the highest nucleotide identity of 96% with strains from Mozambique (MT737707.1), South Africa (MT854762.1) and Brazil (MF161827.1) (Figure 14).

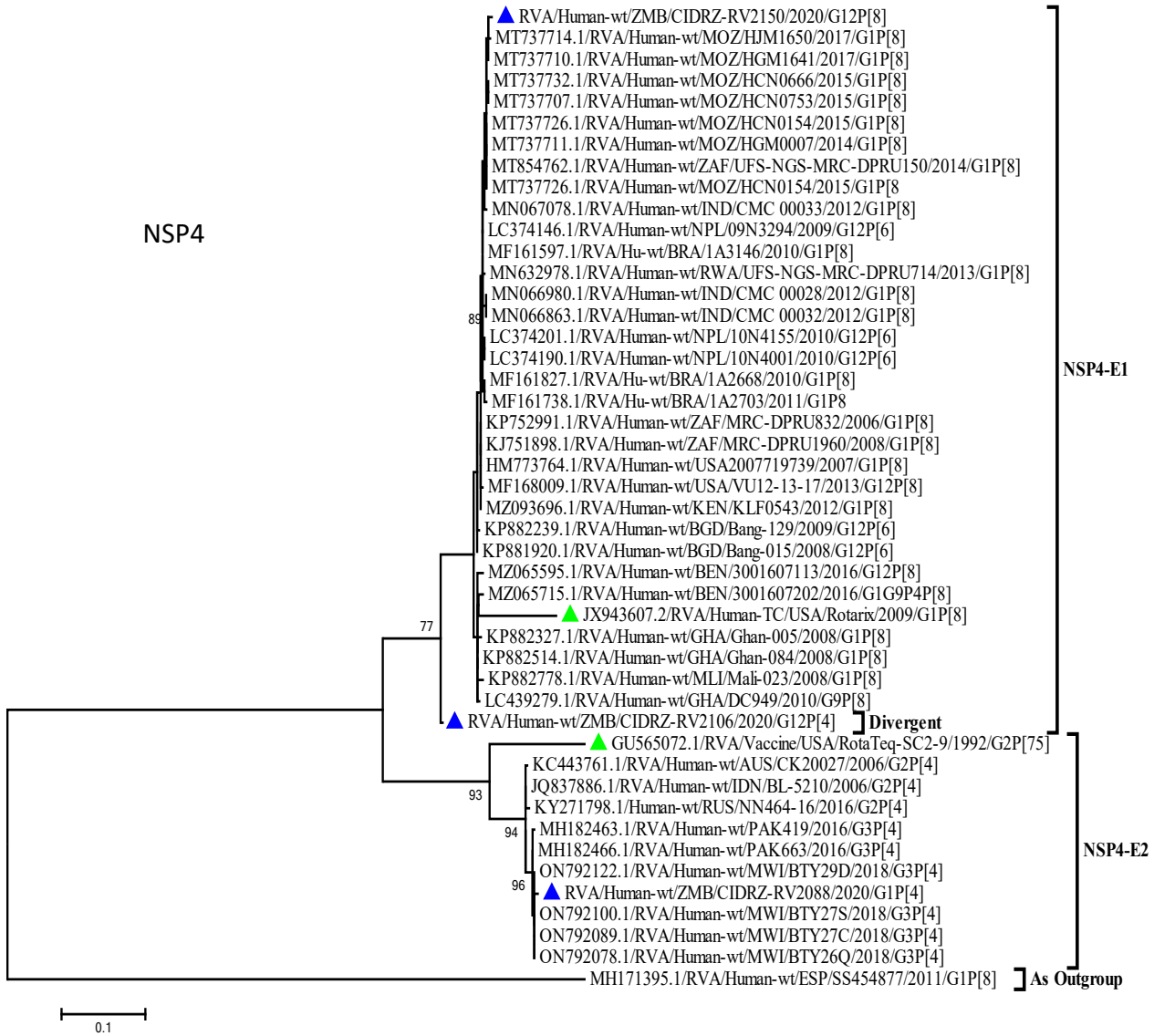

Figure 14: Maximum likelihood phylogenetic tree between the NSP4 gene of the breakthrough strains as well as global strains. Green filled triangles represented vaccine sequences whereas Blue filled triangles indicated Breakthrough strains. Scale at the bottom indicated nucleotide substitutions per site, whilst bootstrap values greater than or equal to 70 were shown on the branches.

4.15 Phylogenetic analysis of NSP5

The NSP5 gene of Wa-like strain CIDRZ-RV2150/2020/G12P[8] clustered in the lineage H1 along with strains from Europe, Asia, the USA, Brazil and Africa with highest shared nucleotide identity of 99% with strains from South Africa (KP752581.1), Brazil (KU361041.1) and Spain (MH171474.1) (Figure 13). The DS-1-like strains CIDRZ-RV2088/2020/G1P[4] and CIDRZ-RV2106/2020/G12P[4] belonged to lineage H2 with highest nucleotide similarity of 99% with strains from Malawi (ON792112.1), South Africa (KJ753786.1), Ghana (LC105587.1) and Pakistan (MH182471.1) (Figure 15).

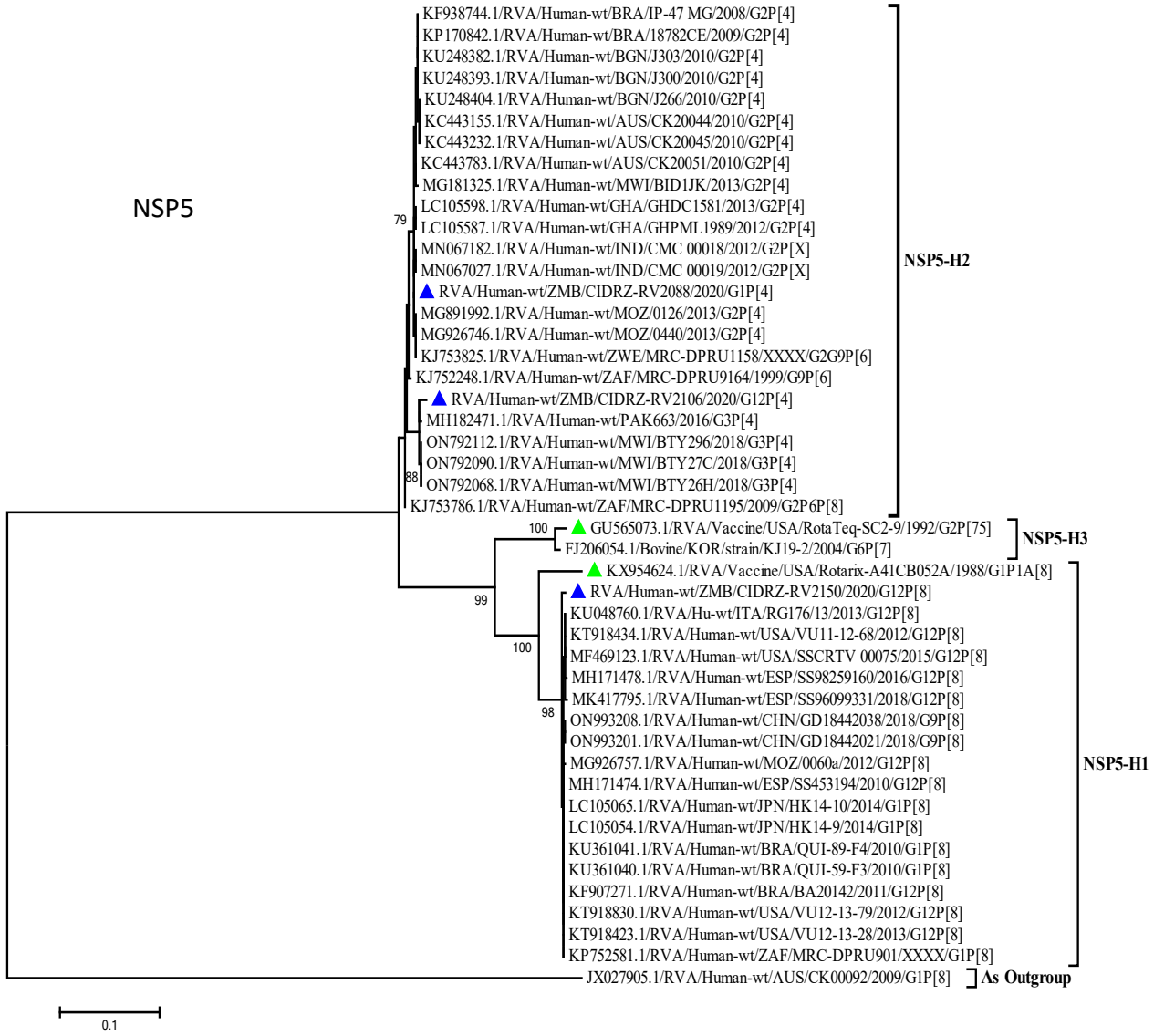

Figure 15: Maximum likelihood phylogenetic tree between the NSP4 gene of the breakthrough strains as well as global strains. Green filled triangles represented vaccine sequences whereas Blue filled triangles indicated Breakthrough strains. Scale at the bottom indicated nucleotide substitutions per site, whilst bootstrap values greater than or equal to 70 were shown on the branches.

CHAPTER FIVE: DISCUSSION AND CONCLUSION

5.1 Discussion

We aimed to characterise the RV strains responsible for causing breakthrough infections using samples from a cohort which had data on vaccination, seroconversion and time to diagnostic of infection post vaccination in children under five years old in Zambia. RV strains causing breakthrough diarrhoeal disease continue to pose an obstacle to further reduction of the disease burden (19). The RV strains detected in the breakthrough diarrhoeal disease were mono reassortant, multiple reassortant and the typical Wa-like strain among fully vaccinated children. The infant infected with mono reassortant RV suggested the reassortment events occurred between the Rotarix vaccine VP7 gene and the wild-type DS-1-like strain. The VP7 gene of the mono reassortant G1P[4] was absolutely identical to the Rotarix vaccine, as well as the Rotarix vaccine-derived strains from Japan(KY616899.1), Belgium (ON855136.1) and the USA (MF469224.1) with shared 99% nucleotide and amino acid identity. A total of 323 days had passed from last receipt of the Rotarix vaccine to the detection of RV, suggesting that the infant was not shedding the Rotarix vaccine, as the reported duration of shedding the vaccine was mainly 6-20 days following last vaccination with peak at 7 days (88). Therefore, the observed vaccine-reassortant suggested to have been acquired from the community circulation and not as a result of vaccine shedding. This finding is consistent with a study from the USA, were a vaccine-reassortant was detected in an infant with acute gastroenteritis (19,89). Clinical trial studies conducted in Malawi and South Africa on the Rotarix vaccine demonstrated that the vaccine induce both a homotypic and heterotypic neutralising antibody response which protected children against development of RV-AGE; although it did not protect against reinfection (90). On the other hand, the analysis of the multiple reassortant strain revealed the exchange of four genes between the Wa-like and DS-1-like strains, indicating an intergenogroup reassortment. The multiple reassortment of genes between the Wa-like and the DS-1-like strains have previous been reported from a study in Rwanda in the post vaccination era (91).

Phylogenetic analysis of the VP7 gene demonstrated the G12 strains clustered in lineage III along with other global strains. This is consistent with finding by Rakau and colleagues which demonstrated that most of African G12 genotypes clustered in lineage III (84). Furthermore, the G12 strains displayed high sequence homology with strains from Mozambique (RVA/Human-wt/MOZ/0289/2012/G12P[6]), Rwanda (RVA/Human-wt/RWA/MRC-DPRU8020/2014/G12P[8]) and South Africa (RVA/Human-wt/ZAF/MRC-DPRU4090/2011/G12P[6]), which indicated local and

regional transmission (91,92). Phylogenetic analysis of VP4 gene revealed the P[4] breakthrough strains belonged to lineage IV along with strains from Malawi, Uganda and Pakistan (87,93). The P[4] strains shared high homology of 99% with human RV strains from Malawi further indicating local and regional circulation. The P[8] breakthrough strain clustered in lineage III distantly from the P[8] Rotarix vaccine clustered in lineage I. The P[8] breakthrough strain was closely related to strains from Mozambique with 99% nucleotide identity, furthermore indicating the transmission between two neighbouring countries. Phylogenetically, 4 segments (VP6, NSP2, NSP3 and NSP4) of strain (CIDRZ-RV2106/2020/G12P[4]) clustered separately from the global strains. In each of the phylogenetic trees, the branching node was supported by strong bootstraps of 73%, 99%, 99%, and 77% respectively. This phenomenon of some of the genes clustering independently from other strains in the lineage was recently reported in the study conducted in Zambia by Nyaga and colleagues were the strain had two segments that clustered separately from the other strains in the lineages (94). It remained unclear to what extent the four distinct clustered genes influenced RV infectivity, as this child did not show any seroconversion to the G1P[8] genotype of the Rotarix vaccine.

The two outer capsid proteins of RV, the VP4 and the VP7, elicited the neutralising antibodies which targeted the antigenic epitope. Therefore, differences in the amino acids between the circulating strains and the vaccine strain in the antigenic epitope might affect the vaccine mediated immune protection (57). The VP7 antigenic epitope of the breakthrough strains were compared with cognate epitope of Rotarix vaccine. All the VP7 antigenic epitope of G1 strain amino acids were conserved in comparison to the Rotarix vaccine. However, the G12 strains had several amino acid differences in comparison to the Rotarix vaccine, which included radical difference such as G96P and M217E. The G96P of which the vaccine had the Glycine which contain a hydrogen side chain, means increased conformational flexibility whereas the proline in the G12 strain indicated restricted conformational flexibility. Furthermore, in the other observed radical variation M217E, methionine was hydrophobic whereas the G12 strains contained glutamate, which is negatively charged (95). The increased number of the amino acid difference observed might affect binding of the vaccine elicited neutralising antibodies against the G12 strains. Our finding was consistent with previous study from the USA, where G12 genotype was predominant among the vaccinated children with RV-AGE and the comparison between the VP 7 component of the vaccine and USA G12 strains revealed several amino acid differences in the antigenic epitope (20).

RV infects mature enterocytes via the proteolytically cleaved VP4 by trypsin into functional subunits the VP5* and VP8*[(34)]. Due to the lower variability in VP4, it has been shown as the component of the vaccine involved in the heterotypic immune response (57). The comparison of the P[4] breakthrough strains and VP4 of vaccine component revealed two amino acids differences which were radical in nature (P114Q and V115T). The P114Q was an immune escape mutation where radical variation was observed, in that Proline contained in the vaccine was nonpolar compared to the polar glutamine contained in the P[4] strains. Furthermore, the hydrophobic valine contained in the vaccine was different to the breakthrough strains which had small polar threonine (95). The observed non-conservative variations might affect the binding of the vaccine elicited antibodies on the antigenic epitopes of the breakthrough strains. It has been shown from previous studies that the neutralising antibodies generated by the VP4 vaccine with the presence of a single VP4 specific antibody to a specific epitope is sufficient to achieve neutralisation in vitro (57). Therefore, the conserved amino acids observed in immune escape positions in this study might play a role in the protection against gastroenteritis.

The study had the limitation of the low cases of RV detected which might be attributed to the passive surveillance in which only children presented at the health facility with diarrhoea were screened for the RV; therefore, children who did not come to the facility might have been missed. The low sensitivity of EIA used in screening might also have missed cases as compared the RT-PCR assay. Despite the noted limitations the study had the noteworthy strength in that it was performed in children with known vaccination history, duration of post vaccination to infection diagnosis as well as the seroconversion data.

5.2 Conclusion

Our data shows the importance of post market surveillance of vaccines, in identifying RV strains responsible for breakthrough infections and characterising the strains to monitor viral evolution to inform next generation of vaccines. We report a strain with 4 gene reassortment which is implicated in breakthrough infections. We also report a reassortment of vaccine strain with DS-1-like wildtype strain. Furthermore, differences observed in amino acids in the VP7 and VP4 antigenic epitopes at immune escape positions might have played a role in the evasion of antibodies elicited by the vaccine.

5.3 Recommendations

Future design of RV vaccines should consider including G12 genotype.

Surveillance should be continued with subsequent WGS for breakthrough genotypes.

References

1. Hallowell BD, Chavers T, Parashar U, Tate JE. Global Estimates of Rotavirus Hospitalizations Among Children Below 5 Years in 2019 and Current and Projected Impacts of Rotavirus Vaccination. Journal of the Pediatric Infectious Diseases Society. 2022 Apr 30;11(4):149–58.

2. Simwaka J, Seheri M, Mulundu G, Kaonga P, Mwenda JM, Chilengi R, et al. Rotavirus breakthrough infections responsible for gastroenteritis in vaccinated infants who presented with acute diarrhoea at University Teaching Hospitals, Children's Hospital in 2016, in Lusaka Zambia. PLoS One. 2021;16(2):e0246025.

3. Ward RL, Bernstein DI, Young EC, Sherwood JR, Knowlton DR, Schiff GM. Human Rotavirus Studies in Volunteers: Determination of Infectious Dose and Serological Response to Infection. Journal of Infectious Diseases. 1986 Nov 1;154(5):871–80.

4. Leung AKC, Kellner JD, Dele Davies H. Rotavirus gastroenteritis. Adv Therapy. 2005 Sep;22(5):476–87.

5. Estes MK, Cohen J. Rotavirus gene structure and function. Microbiol Rev. 1989 Dec;53(4):410–49.

6. Bagchi P, Dutta D, Chattopadhyay S, Mukherjee A, Halder UC, Sarkar S, et al. Rotavirus Nonstructural Protein 1 Suppresses Virus-Induced Cellular Apoptosis To Facilitate Viral Growth by Activating the Cell Survival Pathways during Early Stages of Infection. J Virol. 2010 Jul;84(13):6834–45.

7. Estes MK, Greenberg HB. 2013. Rotaviruses. In: Knipe D, Howley P, editors. Fields virology. Vol. 2. Philadelphia (PA): Lippincott Williams and Wilkins. p. 1347–1401.

8. Argüelles MH, Villegas GA, Castello A, Abrami A, Ghiringhelli PD, Semorile L, et al. VP7 and VP4 Genotyping of Human Group A Rotavirus in Buenos Aires, Argentina. J Clin Microbiol. 2000 Jan;38(1):252–9.

9. Hoshino Y, Kapikian AZ. Classification of rotavirus VP4 and VP7 serotypes. Arch Virol Suppl. 1996;12:99–111.

10. Dóró R, László B, Martella V, Leshem E, Gentsch J, Parashar U, et al. Review of global rotavirus strain prevalence data from six years post vaccine licensure surveillance: is there evidence of strain selection from vaccine pressure? Infect Genet Evol. 2014 Dec;28:446–61.

11. Matthijnssens J, Ciarlet M, Heiman E, Arijs I, Delbeke T, McDonald SM, et al. Full genome-based classification of rotaviruses reveals a common origin between human Wa-Like and porcine rotavirus strains and human DS-1-like and bovine rotavirus strains. J Virol. 2008 Apr;82(7):3204–19.

12. Degiuseppe JI, Beltramino JC, Millán A, Stupka JA, Parra GI. Complete genome analyses of G4P[6] rotavirus detected in Argentinean children with diarrhoea provides evidence of interspecies transmission from swine. Clinical Microbiology and Infection. 2013 Aug;19(8):e367–71.

13. Burnett E, Parashar UD, Tate JE. Global Impact of Rotavirus Vaccination on Diarrhea Hospitalizations and Deaths Among Children <5 Years Old: 2006–2019. The Journal of Infectious Diseases. 2020 Oct 13;222(10):1731–9.

14. https://gskpro.com/content/dam/global/hcpportal/en_US/Prescribing_Information/Rotarix/pdf/ROTARIX-PI-PIL.PDF.

15. https://www.who.int/immunization_standards/vaccine_quality/RotaTeq_Product_Insert.pdf.

16. Gupta S, Tiku VR, Gauhar M, Khatoon K, Ray P. Genetic diversity of G9 rotavirus strains circulating among diarrheic children in North India: A comparison with 116E rotavirus vaccine strain. Vaccine. 2021 Jan 22;39(4):646–51.

17. Naik SP, Zade JK, Sabale RN, Pisal SS, Menon R, Bankar SG, et al. Stability of heat stable, live attenuated Rotavirus vaccine (ROTASIIL®). Vaccine. 2017 May;35(22):2962–9.

18. Kaneko M, Takanashi S, Thongprachum A, Hanaoka N, Fujimoto T, Nagasawa K, et al. Identification of vaccine-derived rotavirus strains in children with acute gastroenteritis in Japan, 2012-2015. PLoS One. 2017;12(9):e0184067.

19. Simsek C, Bloemen M, Jansen D, Beller L, Descheemaeker P, Reynders M, et al. High Prevalence of Coinfecting Enteropathogens in Suspected Rotavirus Vaccine Breakthrough Cases. Diekema DJ, editor. J Clin Microbiol. 2021 Nov 18;59(12):e01236-21.

20. Ogden KM, Tan Y, Akopov A, Stewart LS, McHenry R, Fonnesbeck CJ, et al. Multiple Introductions and Antigenic Mismatch with Vaccines May Contribute to Increased Predominance of G12P[8] Rotaviruses in the United States. López S, editor. J Virol. 2019 Jan;93(1):e01476-18.

21. Day T, Kennedy DA, Read AF, Gandon S. Pathogen evolution during vaccination campaigns. PLoS Biol. 2022 Sep;20(9):e3001804.

22. Seheri M, Nemarude L, Peenze I, Netshifhefhe L, Nyaga MM, Ngobeni HG, et al. Update of Rotavirus Strains Circulating in Africa From 2007 Through 2011. Pediatric Infectious Disease Journal. 2014 Jan;33(Supplement 1):S76–84.

23. Troeger C, Khalil IA, Rao PC, Cao S, Blacker BF, Ahmed T, et al. Rotavirus Vaccination and the Global Burden of Rotavirus Diarrhea Among Children Younger Than 5 Years. JAMA Pediatr. 2018 Oct 1;172(10):958–65.

24. Svensson L, Sheshberadaran H, Vesikari T, Norrby E, Wadell G. Immune response to rotavirus polypeptides after vaccination with heterologous rotavirus vaccines (RIT 4237, RRV-1). J Gen Virol. 1987 Jul;68 (Pt 7):1993–9.

25. Mihalov-Kovács E, Gellért Á, Marton S, Farkas SL, Fehér E, Oldal M, et al. Candidate new rotavirus species in sheltered dogs, Hungary. Emerg Infect Dis. 2015 Apr;21(4):660–3.

26. Bányai K, Kemenesi G, Budinski I, Földes F, Zana B, Marton S, et al. Candidate new rotavirus species in Schreiber's bats, Serbia. Infect Genet Evol. 2017 Mar;48:19–26.

27. Angel J,. Greenberg H.B, in Encyclopedia of Virology (Third Edition), 2008.

28. Catherine Yen. Principles and Practice of Pediatric Infectious Diseases (Fourth Edition), 2012.

29. Coluchi N, Munford V, Manzur J, Vazquez C, Escobar M, Weber E, et al. Detection, Subgroup Specificity, and Genotype Diversity of Rotavirus Strains in Children with Acute Diarrhea in Paraguay. J Clin Microbiol. 2002 May;40(5):1709–14.

30. Hoshino Y, Sereno MM, Midthun K, Flores J, Kapikian AZ, Chanock RM. Independent segregation of two antigenic specificities (VP3 and VP7) involved in neutralization of rotavirus infectivity. Proc Natl Acad Sci U S A. 1985 Dec;82(24):8701–4.

31. Todd S, Page NA, Duncan Steele A, Peenze I, Cunliffe NA. Rotavirus Strain Types Circulating in Africa: Review of Studies Published during 1997–2006. J INFECT DIS. 2010 Sep;202(S1):S34–42.

32. Esona MD, Gautam R, Katz E, Jaime J, Ward ML, Wikswo ME, et al. Comparative genomic analysis of genogroup 1 and genogroup 2 rotaviruses circulating in seven US cities, 2014–2016. Virus Evolution. 2021 Jan 20;7(1): veab023.

33. Bishop RuthF, Davidson GP, Holmes IH, Ruck BJ. VIRUS PARTICLES IN EPITHELIAL CELLS OF DUODENAL MUCOSA FROM CHILDREN WITH ACUTE NON-BACTERIAL GASTROENTERITIS. The Lancet. 1973 Dec;302(7841):1281–3.

34. Jayaram H, Estes MK, Prasad BVV. Emerging themes in rotavirus cell entry, genome organization, transcription and replication. Virus Res. 2004 Apr;101(1):67–81.

35. Mathieu M, Petitpas I, Navaza J, Lepault J, Kohli E, Pothier P, et al. atomic structure of the major capsid protein of rotavirus: implications for the architecture of the virion. EMBO J. 2001 Apr 2;20(7):1485–97.

36. Charpilienne A, Lepault J, Rey F, Cohen J. Identification of rotavirus VP6 residues located at the interface with VP2 that are essential for capsid assembly and transcriptase activity. J Virol. 2002 Aug;76(15):7822–31.

37. Desselberger U. Rotaviruses. Virus Research. 2014 Sep; 190:75–96.

38. Padilla-Noriega L, Dunn SJ, López S, Greenberg HB, Arias CF. Identification of two independent neutralization domains on the VP4 trypsin cleavage products VP5* and VP8* of human rotavirus ST3. Virology. 1995 Jan;206(1):148–54.

39. Settembre EC, Chen JZ, Dormitzer PR, Grigorieff N, Harrison SC. Atomic model of an infectious rotavirus particle: Atomic model of an infectious rotavirus particle. The EMBO Journal. 2011 Jan 19;30(2):408–16.

40. Tortorici MA, Shapiro BA, Patton JT. A base-specific recognition signal in the 5' consensus sequence of rotavirus plus-strand RNAs promotes replication of the double-stranded RNA genome segments. RNA. 2006 Jan;12(1):133–46.

41. Komoto S, Kanai Y, Fukuda S, Kugita M, Kawagishi T, Ito N, et al. Reverse Genetics System Demonstrates that Rotavirus Nonstructural Protein NSP6 Is Not Essential for Viral Replication in Cell Culture. Dermody TS, editor. J Virol. 2017 Nov;91(21):e00695-17.

42. Lundgren O, Svensson L. Pathogenesis of rotavirus diarrhea. Microbes Infect. 2001 Nov;3(13):1145–56.

43. Arias CF, Silva-Ayala D, López S. Rotavirus Entry: a Deep Journey into the Cell with Several Exits. Tsai B, editor. J Virol. 2015 Jan 15;89(2):890–3.

44. Dormitzer PR, Nason EB, Prasad BVV, Harrison SC. Structural rearrangements in the membrane penetration protein of a non-enveloped virus. Nature. 2004 Aug 26;430(7003):1053–8.

45. Papa G, Borodavka A, Desselberger U. Viroplasms: Assembly and Functions of Rotavirus Replication Factories. Viruses. 2021 Jul 12;13(7):1349.

46. Donato CM, Ch'ng LS, Boniface KF, Crawford NW, Buttery JP, Lyon M, et al. Identification of strains of RotaTeq rotavirus vaccine in infants with gastroenteritis following routine vaccination. J Infect Dis. 2012 Aug 1;206(3):377–83.

47. Crawford SE, Criglar JM, Liu Z, Broughman JR, Estes MK. COPII Vesicle Transport Is Required for Rotavirus NSP4 Interaction with the Autophagy Protein LC3 II and Trafficking to Viroplasms. López S, editor. J Virol. 2019 Dec 12;94(1):e01341-19.

48. Ansari SA, Springthorpe VS, Sattar SA. Survival and Vehicular Spread of Human Rotaviruses: Possible Relation to Seasonality of Outbreaks. Clinical Infectious Diseases. 1991 May 1;13(3):448–61.

49. Uhnoo I, Olding-Stenkvist E, Kreuger A. Clinical features of acute gastroenteritis associated with rotavirus, enteric adenoviruses, and bacteria. Archives of Disease in Childhood. 1986 Aug 1;61(8):732–8.

50. Eskilsson A, Mirrasekhian E, Dufour S, Schwaninger M, Engblom D, Blomqvist A. Immune-Induced Fever Is Mediated by IL-6 Receptors on Brain Endothelial Cells Coupled to STAT3-Dependent Induction of Brain Endothelial Prostaglandin Synthesis. J Neurosci. 2014 Nov 26;34(48):15957–61.

51. Crawford SE, Ramani S, Tate JE, Parashar UD, Svensson L, Hagbom M, et al. Rotavirus infection. Nat Rev Dis Primers. 2017 Nov 9;3(1):17083.

52. Ball JM, Tian P, Zeng CQ, Morris AP, Estes MK. Age-dependent diarrhea induced by a rotaviral nonstructural glycoprotein. Science. 1996 Apr 5;272(5258):101–4.

53. Hagbom M, Hellysaz A, Istrate C, Nordgren J, Sharma S, de-Faria FM, et al. The 5-HT $_3$ Receptor Affects Rotavirus-Induced Motility. López S, editor. J Virol. 2021 Jul 12;95(15):e00751-21.

54. Sen A, Ding S, Greenberg HB. The Role of Innate Immunity in Regulating Rotavirus Replication, Pathogenesis, and Host Range Restriction and the Implications for Live Rotaviral Vaccine Development. In: Mucosal Vaccines [Internet]. Elsevier; 2020 [cited 2023 Aug 30]. p. 683–97. Available from: https://linkinghub.elsevier.com/retrieve/pii/B9780128119242000419

55. Cerutti A, Rescigno M. The biology of intestinal immunoglobulin A responses. Immunity. 2008 Jun;28(6):740–50.

56. Angel J, Steele AD, Franco MA. Correlates of protection for rotavirus vaccines: Possible alternative trial endpoints, opportunities, and challenges. Human Vaccines & Immunotherapeutics. 2014 Dec 2;10(12):3659–71.

57. Nair N, Feng N, Blum LK, Sanyal M, Ding S, Jiang B, et al. VP4- and VP7-specific antibodies mediate heterotypic immunity to rotavirus in humans. Sci Transl Med. 2017 Jun 21;9(395):eaam5434.

58. Malm M, Hyöty H, Knip M, Vesikari T, Blazevic V. Development of T cell immunity to norovirus and rotavirus in children under five years of age. Sci Rep. 2019 Mar 1;9(1):3199.

59. Vesikari T, Matson DO, Dennehy P, Van Damme P, Santosham M, Rodriguez Z, et al. Safety and efficacy of a pentavalent human-bovine (WC3) reassortant rotavirus vaccine. N Engl J Med. 2006 Jan 5;354(1):23–33.

60. Heaton PM, Goveia MG, Miller JM, Offit P, Clark HF. Development of a Pentavalent Rotavirus Vaccine against Prevalent Serotypes of Rotavirus Gastroenteritis. J INFECT DIS. 2005 Sep;192(s1):S17–21.

61. Ruiz-Palacios GM, Pérez-Schael I, Velázquez FR, Abate H, Breuer T, Clemens SC, et al. Safety and Efficacy of an Attenuated Vaccine against Severe Rotavirus Gastroenteritis. N Engl J Med. 2006 Jan 5;354(1):11–22.

62. Chilengi R, Mwila- Kazimbaya K, Chirwa M, Sukwa N, Chipeta C, Velu RM, et al. Immunogenicity and safety of two monovalent rotavirus vaccines, ROTAVAC® and ROTAVAC 5D® in Zambian infants. Vaccine. 2021 Jun;39(27):3633–40.

63. Kulkarni PS, Desai S, Tewari T, Kawade A, Goyal N, Garg BS, et al. A randomized Phase III clinical trial to assess the efficacy of a bovine-human reassortant pentavalent rotavirus vaccine in Indian infants. Vaccine. 2017 Oct 27;35(45):6228–37.

64. Seheri LM, Magagula NB, Peenze I, Rakau K, Ndadza A, Mwenda JM, et al. Rotavirus strain diversity in Eastern and Southern African countries before and after vaccine introduction. Vaccine. 2018 Nov 12;36(47):7222–30.

65. Yandle Z, Coughlan S, Dean J, Tuite G, Conroy A, De Gascun CF. Group A Rotavirus Detection and Genotype Distribution before and after Introduction of a National Immunisation Programme in Ireland: 2015–2019. Pathogens. 2020 Jun 7;9(6):449.

66. Nyaga MM, Jere KC, Esona MD, Seheri ML, Stucker KM, Halpin RA, et al. Whole genome detection of rotavirus mixed infections in human, porcine and bovine samples co-infected with various rotavirus strains collected from sub-Saharan Africa. Infection, Genetics and Evolution. 2015 Apr;31:321–34.

67. Bishop RF, Barnes GL, Cipriani E, Lund JS. Clinical immunity after neonatal rotavirus infection. A prospective longitudinal study in young children. N Engl J Med. 1983 Jul 14;309(2):72–6.

68. Velázquez FR, Matson DO, Calva JJ, Guerrero L, Morrow AL, Carter-Campbell S, et al. Rotavirus infection in infants as protection against subsequent infections. N Engl J Med. 1996 Oct 3;335(14):1022–8.

69. Ward RL. Rotavirus vaccines: how they work or don't work. Expert Rev Mol Med. 2008 Feb 12;10:e5.

70. Laban NM, Bosomprah S, Simuyandi M, Chibuye M, Chauwa A, Chirwa-Chobe M, et al. Evaluation of ROTARIX® Booster Dose Vaccination at 9 Months for Safety and Enhanced Anti-Rotavirus Immunity in Zambian Children: A Randomised Controlled Trial. Vaccines (Basel). 2023 Feb 3;11(2):346.

71. QIAamp Viral RNA Mini Handbook 07/2020.

72. Zeller M, Patton JT, Heylen E, De Coster S, Ciarlet M, Van Ranst M, et al. Genetic analyses reveal differences in the VP7 and VP4 antigenic epitopes between human rotaviruses circulating in Belgium and rotaviruses in Rotarix and RotaTeq. J Clin Microbiol. 2012 Mar;50(3):966–76.

73. Magagula NB, Esona MD, Nyaga MM, Stucker KM, Halpin RA, Stockwell TB, et al. Whole genome analyses of G1P[8] rotavirus strains from vaccinated and non-vaccinated South African children presenting with diarrhea. J Med Virol. 2015 Jan;87(1):79–101.

74. Oskari P. Rotavirus Whole Genome Sequencing with Next-Generation Sequencing. Report No.: 10024/101134.

75. illumina. Illumina DNA Prep reference guide.

76. (https://www.geneious.com)Geneious Prime.

77. Olson RD, Assaf R, Brettin T, Conrad N, Cucinell C, Davis JJ, et al. Introducing the Bacterial and Viral Bioinformatics Resource Center (BV-BRC): a resource combining PATRIC, IRD and ViPR. Nucleic Acids Res. 2023 Jan 6;51(D1):D678–89.

78. Sayers EW, Beck J, Bolton EE, Bourexis D, Brister JR, Canese K, et al. Database resources of the National Center for Biotechnology Information. Nucleic Acids Research. 2021 Jan 8;49(D1):D10–7.

79. Tamura K, Stecher G, Peterson D, Filipski A, Kumar S. MEGA6: Molecular Evolutionary Genetics Analysis Version 6.0. Molecular Biology and Evolution. 2013 Dec;30(12):2725–9.

80. Tamura K, Peterson D, Peterson N, Stecher G, Nei M, Kumar S. MEGA5: molecular evolutionary genetics analysis using maximum likelihood, evolutionary distance, and maximum parsimony methods. Mol Biol Evol. 2011 Oct;28(10):2731–9.

81. Posada D, Buckley TR. Model Selection and Model Averaging in Phylogenetics: Advantages of Akaike Information Criterion and Bayesian Approaches Over Likelihood Ratio Tests. Thorne J, editor. Systematic Biology. 2004 Oct 1;53(5):793–808.

82. Siqueira JD, Dominguez-Bello MG, Contreras M, Lander O, Caballero-Arias H, Xutao D, et al. Complex virome in feces from Amerindian children in isolated Amazonian villages. Nat Commun. 2018 Oct 15;9(1):4270.

83. Mullick S, Mukherjee A, Ghosh S, Pazhani GP, Sur D, Manna B, et al. Community based case-control study of rotavirus gastroenteritis among young children during 2008-2010 reveals vast genetic diversity and increased prevalence of G9 strains in Kolkata. PLoS One. 2014;9(11):e112970.

84. Rakau KG, Nyaga MM, Gededzha MP, Mwenda JM, Mphahlele MJ, Seheri LM, et al. Genetic characterization of G12P[6] and G12P[8] rotavirus strains collected in six African countries between 2010 and 2014. BMC Infect Dis. 2021 Dec;21(1):107.

85. Ludert JE, Ruiz MC, Hidalgo C, Liprandi F. Antibodies to rotavirus outer capsid glycoprotein VP7 neutralize infectivity by inhibiting virion decapsidation. J Virol. 2002 Jul;76(13):6643–51.

86. Heiman EM, McDonald SM, Barro M, Taraporewala ZF, Bar-Magen T, Patton JT. Group A human rotavirus genomics: evidence that gene constellations are influenced by viral protein interactions. J Virol. 2008 Nov;82(22):11106–16.

87. Sadiq A, Bostan N, Bokhari H, Yinda KC, Matthijnssens J. Whole Genome Analysis of Selected Human Group A Rotavirus Strains Revealed Evolution of DS-1-Like Single- and Double-Gene Reassortant Rotavirus Strains in Pakistan During 2015–2016. Front Microbiol. 2019 Nov 14;10:2641.

88. Hsieh YC, Wu FT, Hsiung CA, Wu HS, Chang KY, Huang YC. Comparison of virus shedding after lived attenuated and pentavalent reassortant rotavirus vaccine. Vaccine. 2014 Feb;32(10):1199–204.

89. Boom JA, Sahni LC, Payne DC, Gautam R, Lyde F, Mijatovic-Rustempasic S, et al. Symptomatic Infection and Detection of Vaccine and Vaccine-Reassortant Rotavirus Strains in 5 Children: A Case Series. Journal of Infectious Diseases. 2012 Oct 15;206(8):1275–9.

90. Steele AD, Neuzil KM, Cunliffe NA, Madhi SA, Bos P, Ngwira B, et al. Human rotavirus vaccine Rotarix™ provides protection against diverse circulating rotavirus strains in African infants: a randomized controlled trial. BMC Infect Dis. 2012 Sep 13;12:213.

91. Rasebotsa S, Uwimana J, Mogotsi MT, Rakau K, Magagula NB, Seheri ML, et al. Whole-Genome Analyses Identifies Multiple Reassortant Rotavirus Strains in Rwanda Post-Vaccine Introduction. Viruses. 2021 Jan 12;13(1):95.

92. Strydom A, João ED, Motanyane L, Nyaga MM, Christiaan Potgieter A, Cuamba A, et al. Whole genome analyses of DS-1-like Rotavirus A strains detected in children with acute diarrhoea in southern Mozambique suggest several reassortment events. Infection, Genetics and Evolution. 2019 Apr;69:68–75.

93. Mhango C, Banda A, Chinyama E, Mandolo JJ, Kumwenda O, Malamba-Banda C, et al. Comparative whole genome analysis reveals re-emergence of human Wa-like and DS-1-like G3 rotaviruses after Rotarix vaccine introduction in Malawi. Virus Evol. 2023;9(1):vead030.

94. Maringa WM, Simwaka J, Mwangi PN, Mpabalwani EM, Mwenda JM, Mphahlele MJ, et al. Whole Genome Analysis of Human Rotaviruses Reveals Single Gene Reassortant Rotavirus Strains in Zambia. Viruses. 2021 Sep 18;13(9):1872.

95. Barnes MR, Gray IC. Bioinformatics for geneticists. Chichester, West Sussex, England ; Hoboken, N.J: Wiley; 2003. 408 p.

Addenda

Addendum 1: Ethics Approval from University of Zambia Biological Research Ethics Committee

UNIVERSITY OF ZAMBIA
BIOMEDICAL RESEARCH ETHICS COMMITTEE

Telephone: +260977925304
Telegrams: UNZA, LUSAKA
Telex: UNZALU ZA 44370
Fax: + 260-1-250753

Ridgeway Campus
P.O. Box 50110
Lusaka, Zambia
E-mail: unzarec@unza.zm

Federal Assurance No. FWA00000338 **IRB00001131 of IORG0000774** **NHRAR-REC No 2021-05-0002**

19th December 2022

Your REF. No. 3569-2022

Mr. Innocent Mwape,
University Teaching Hospitals,
Children's Hospital,
Lusaka.

Dear Mr. Mwape,

RE: WHOLE GENOME ANALYSIS OF ROTAVIRUS CIRCULATING IN ZAMBIA BEFORE AND AFTER VACCINATION TO UNDERSTAND THE BREAKTHROUGH STRAINS CAUSING SEVERE GASTROENTERITIS IN CHILDREN UNDER FIVE YEARS (REF. NO. 3569-2022)

Your application for a waiver of ethics review for the aforementioned study was reviewed. The **waiver** is hereby **granted**. The approval was conducted in line with the University of Zambia Biomedical Research Ethics Committee guidelines on granting waiver of Ethics review.

Date of approval: 19th December 2022 **Date of expiry: 18th December 2023**

CONDITIONS:

i. The waiver is based strictly on your submitted proposal. Should there be need for you to modify or make changes to the proposal; you will need to seek clearance from the Biomedical Research Ethics Committee.
ii. This waiver does not release you from the obligation of ensuring confidentiality.
iii. If you need any clarifications please consult this office.
iv. **NHRA:** You are advised to obtain final study clearance and approval to conduct research in Zambia from the National Health Research Authority (NHRA) before commencing the research project.
v. Ensure that a final copy of the results is submitted to this Committee.

Yours sincerely,

Sody Mweetwa Munsaka, BSc., MSc., PhD
CHAIRPERSON

THE NATIONAL HEALTH RESEARCH AUTHORITY
Paediatric Centre of Excellence
University Teaching Hospital
P.O. Box 30075
LUSAKA
Telephone: +260 211 250309 | **Mobile:** +260 95 5632726
Email: znhrasec@gmail.com | **Website:** www.nhra.org.zm

Dr. Izukanji Sikazwe
Chief Executive Officer, CIDRZ
Centre for Infectious Disease Research in Zambia
Plot # 34620 Off Alick Nkhata Road, Mass Media,
P.O. Box 34681
LUSAKA

CIDRZ CENTRE FOR INFECTIOUS DISEASE RESEARCH IN ZAMBIA
RECEIVED
13 JUN 2018

11th June, 2018.

Dear Dr. Sikazwe,

RE: REQUEST FOR PERMISSION TO CONDUCT A STUDY

The National Health Research Ethics Board (NHREB) is in receipt of your request for permission to conduct study entitled "**A randomised controlled trial of two versus three doses of Rotarix™ vaccine for boosting and longevity of vaccine immune responses in Zambia (ROVAS-2)**".

The NHREB has no objection to your request on condition that:

1. **A Material Transfer Agreement is obtained and cleared by the National Health Research Ethics Board for all samples to be sent outside the country for analysis.**
2. The relevant Provincial and District Medical Officers where the study is being conducted. are fully appraised;
3. Progress updates are provided to NHRA quarterly from the date of commencement of the study;
4. The final study report is cleared by the NHRA before any publication or dissemination within or outside the country;
5. After clearance for publication or dissemination by the NHRA, the final study report is shared with all relevant Provincial and District Directors of Health where the study was being conducted, University leadership, and all key respondents.

Yours sincerely,

REPUBLIC OF ZAMBIA
NATIONAL HEALTH RESEARCH AUTHORITY
12 JUN 2018
OFFICE OF THE DIRECTOR/CEO
P.O. BOX 30075
LUSAKA

Prof. Patrick Musonda
Chairperson,
National Health Research Ethics Board

All correspondences should be addressed to the Director and Chief Executive Officer

Addendum 2: G12 strains (CIDRZ-RV2150 G12P[4] and CIDRZ-RV2106G12P[8]) shared 100% nucleotide identity

	Nucleotide percentage Identity											
	JN849114.1/	KY61689	MG571803.1	ON855124.1/	KC579492.1/	CIDRZ-RV2088 G1P[4]	DQ204743.1/	AB071404.1/	CIDRZ-RV2106 G12P[4]	CIDRZ-RV2150 G12P[8]	KM008668	OQ133292.1/
JN849114.1/RVA/Vaccine/USA/Rotarix-A41CB052A/1988/G1P1A[8]		100	100	99.847	99.693	99.796	74.029	74.029	74.54	74.54	73.824	73.211
KY616899.1/RVA/Human-wt/JPN/IP11786/2013/G1P[8]	100		100	99.847	99.707	99.798	75.361	75.361	74.54	74.85	74.194	73.211
MG571803.1/RVA/Human-wt/VEN/VME8A/2015/G1P[8]	100	100		99.847	99.701	99.798	74.576	74.576	74.54	74.699	74.089	73.211
MN478595.1/RVA/Human-wt/USA/3000371148/2015/G1P[8]	99.898	99.898	99.898	99.745	99.592	99.694	74.21	74.21	74.642	74.72	74.006	73.313
KC580519.1/RVA/Human-wt/USA/DC4084/1988/G1P[8]	99.591	99.609	99.601	99.439	99.707	99.393	75.073	75.073	74.642	74.799	74.294	73.415
CIDRZ-RV2088G1P[4]	99.796	99.798	99.798	99.643	99.494		74.089	74.089	74.438	74.595	73.802	73.108
DQ377572.1/RVA/ITA/Human-wt/PA78/89/2006/G1P[8]	97.046	97.046	97.046	96.888	96.941	97.046	73.207	72.996	73.523	73.523	72.89	74.051
DQ492674.1/RVA/Human-wt/BGD/Dhaka16/2003/G1P[8]	93.661	94.033	93.819	93.527	94.037	93.522	75.424	75.33	74.029	74.455	73.589	73.313
MZ027445.1/RVA/Human-wt/ZMB/DPRU13541/2016/G1P[8]	93.456	93.489	93.489	93.323	93.795	93.786	73.957	74.669	74.847	74.975	74.312	73.313
KJ752243.1/RVA/Human-wt/ZMB/MRC-DPRU1648/2009/G1P[8]	94.07	94.33	94.217	93.935	94.428	93.977	74.682	74.487	74.233	74.398	73.79	74.131
MG181496.1/RVA/Human-wt/MWI/BID110/2012/G1P[8]	94.376	94.706	94.516	94.241	94.721	94.231	75.33	75.518	74.131	74.455	73.69	73.824
KP752676.1/RVA/Human-wt/SWZ/MRC-DPRU4550/2010/G1P[8]	93.865	94.135	94.018	93.731	94.233	93.775	74.487	74.78	74.335	74.498	73.891	73.211
AB018697.1/RVA/Human-wt/JPN/AU19/1999/G1P[8]	87.117	87.156	87.156	87.105	87.462	86.952	75.127	74.516	74.131	74.21	74.108	72.393
L24164.1/RVA/Human-wt/ITA/10913/1994/G1	85.174	85.811	85.543	85.066	85.924	85.121	73.926	73.543	73.517	73.774	73.286	72.188
M92651.1/RVA/Bovine-wt/rotavirus/USA/1993/G1	84.765	85.178	84.945	84.76	85.435	84.717	74.2	73.54	73.722	74.257	73.387	71.779
MG58290.1/RVA/Human-wt/strain-L26/JPN/2016/G12P[8]	73.62	74.687	74.078	73.649	74.682	73.684	91.808	90.96	89.775	89.604	89.617	72.29
EF672595.1/RVA/Human-wt/strain-L26/JPN/2008/G12P[8]	73.824	73.904	73.904	73.853	74.21	73.802	92.151	91.233	90.389	90.418	90.112	71.984
DQ204743.1/Pig-wt/IND/RU172/2002/G12P[7]	74.029	75.361	74.576	74.057	75.269	74.089		89.831	89.059	89.208	88.609	73.824
AB071404.1/RVA/Human-wt/Strain-T152/THA/2002/G12P[9]	74.029	75.361	74.576	73.955	75.073	74.089	89.831		96.217	95.941	96.069	71.37
KF006878.2/RVA/Hu-wt/RUS/Novosibirsk/Nov12-N4489/2012/G12P[8]	74.54	75.369	75.075	74.465	75.322	74.595	89.971	96.592	98.773	98.614	98.589	72.29
CIDRZ-RV2106 G12P[4]	74.54	74.54	74.54	74.387	74.642	74.438	89.059	96.217		100	98.16	72.29
CIDRZ-RV2150 G12P[8]	74.54	74.85	74.699	74.465	74.799	74.595	89.208	95.941	100		98.165	72.29
KM008668.1/RVA/Human-wt/IND/KOL-24-09/2009/G12P[6]	73.824	74.194	74.089	73.751	74.294	73.802	88.609	96.069	98.16	98.165		71.677
OQ133292.1/RVA/Human-wt/ZMB/-DPRU4819/2014/G2P[4]	73.211	73.211	73.211	73.16	73.517	73.108	73.824	71.37	72.29	72.29	71.677	